

# Oligocene archaeomonad stomatocysts from the Polish Central Paratethys

IRENA KACZMARSKA, JAMES M. EHRMAN, and BRAJOGOPAL SAMANTA



Kaczmarska, I., Ehrman, J.M., and Samanta, B. 2025. Oligocene archaeomonad stomatocysts from the Polish Central Paratethys. *Acta Palaeontologica Polonica* 70 (2): 385–410.

An unanticipated diversity of archaeomonad stomatocysts intermixed with marine plankton including diatoms, silicoflagellates, pormaleans and individual siliceous protistan scales was encountered in Rupelian diatomites from the Central Paratethys. In this initial report we document 27 previously described species attributed to three palaeomorphogenera (*Archaeomonas*, *Archaeosphaeridium*, and *Litheusphaerella*). An additional eight morphospecies from two genera (*Archaeomonas anterioconica* Kaczmarska sp. nov., *A. asharya* Samanta sp. nov., *A. genetynanii* Ehrman sp. nov., *A. jimstehrii* Ehrman & Kaczmarska sp. nov., *A. lenistriata* Kaczmarska sp. nov., *A. litheusphaerellamima* Samanta sp. nov., *A. sextapapillatus* Kaczmarska sp. nov., and *Litharchaeocystis centparatethianus* Ehrman sp. nov.) are proposed as new to science. We also found at least a dozen more distinct morphotypes in orientations and quantities insufficient for formal description that will be the subject of further studies. Our report is the first from the Central Paratethys and the most species rich archaeomonad flora reported from the Oligocene worldwide. The combination of previously described archaeomonad species recovered with the associated diatoms, pormaleans, silicoflagellates, ebridians, and other marine biota suggest that our stomatocysts are native to their basin and inhabited the neritic part of the Paratethys. Unfortunately, the small number of dedicated studies and archaeomonad species known to date still hampers a better understanding of their biostratigraphy and paleoecology.

**Key words:** Chrysophyta, Haptophyta, Archaeomonadaceae, *Archaeomonas*, *Archaeosphaeridium*, *Litheusphaerella*, diatomites, siliceous nannofossils, stomatocyst, Rupelian, Oligocene, Polish Flysch Carpathians.

Irena Kaczmarska [ihrman@mta.ca; ORCID: <https://orcid.org/0000-0002-2527-6148>], Biology Department, Mount Allison University, Sackville, New Brunswick, E4L 1G7, Canada.

James M. Ehrman [jehrm@mta.ca; ORCID: <https://orcid.org/0000-0001-7428-2651>], Digital Microscopy Facility, Mount Allison University, Sackville, New Brunswick, E4L 1G7, Canada.

Brajogopal Samanta [brajomicro@gmail.com; ORCID: <https://orcid.org/0000-0003-1110-5097>], Department of Life Sciences, GITAM School of Science, GITAM, Rushikonda, Visakhapatnam, Andhra Pradesh 530045, India.

Received 23 October 2024, accepted 16 April 2025, published online 30 June 2025.

Copyright © 2025 I. Kaczmarska et al. This is an open-access article distributed under the terms of the Creative Commons Attribution License (for details please see <http://creativecommons.org/licenses/by/4.0/>), which permits unrestricted use, distribution, and reproduction in any medium, provided the original author and source are credited.

## Introduction

The family Archaeomonadaceae Deflandre, 1932c, was erected to accommodate fossilised cell walls of the chrysophycean-like stomatocysts found in marine sediments. They could not be attributed to modern, predominantly freshwater genera (Tynan 1960) since their classification is based on living vegetative cells. Archaeomonadaceae were described and named following the binomial Linnaean convention. Although admitted being artificial by its creator, Deflandre (1932c) erected his system to facilitate future studies of such remains. Indeed, it has been a common and needed practice in palaeontology for extinct, partially preserved fossils to be assigned specific scientific names until such time when

complete specimens, entire life cycles and non-mineralised remains are recovered. Recognising that fossilised biological remains generally do not present complete organisms or all of their life cycle stages, such practice is permitted under the International Code of Nomenclature for algae, fungi, and plants (ICN Shenzhen Code; Turland et al. 2018: articles 1.2 and 11.1).

Archaeomonads were thought to be extinct until morphologically similar living marine forms were discovered. They were first found in environments associated with modern sea-ice (Mitchell and Silver 1982; Riaux-Gobin and Stumm 2006; Riaux-Gobin et al. 2011), although it is unlikely that they lived under similar conditions in the Cretaceous or Paleogene oceans. Stomatocysts, which are widely considered resting stages of chrysophyceans, are also referred to as

statospores, stomatospores, statocysts (Sandgren 1988; Duff et al. 1995), or simply siliceous cysts.

In lacustrine sediments, chrysophycean stomatocysts are known since the Triassic (~228–235 Ma; Zhang et al. 2016), where they already demonstrate considerable diversity and complexity of wall structures. The earliest known stomatocysts from marine sediments are Early Cretaceous in age (~125 Ma; Harwood and Gersonde 1990). They have been found worldwide in Upper Cretaceous and Cenozoic sediments, although generally as a small addition to the total abundance of other siliceous microfossils. Consequently, archaeomonad biostratigraphy is relatively undeveloped (Tynan 1971; Lipps 1993). Diverse assemblages of fossilised archaeomonads are spotty, the best known are those from the Cretaceous, Eocene, and Miocene (Table 1). In contrast to general abundance, archaeomonad morphological diversity is high. Nearly every publication on the subject reports at least several species new to science (Hajós 1968; Perch-Nielsen 1978; Riaux-Gobin and Stumm 2006; Kato 2019). Furthermore, when more abundant, archaeomonads have been found to be ecologically informative for marine palaeoenvironments (Stickley et al. 2008; Kato and Suto 2019), similar to their freshwater counterparts (Wilkinson et al. 1999).

Extrapolating from extant freshwater chrysophytes, one individual living cell produces one endogenous cyst with a silicified, nearly continuous cell wall. Stomatocysts have only one small opening (pore) which is used by the

enclosed protoplast to exit the cyst. The pores are closed by an infrequently fossilised plug. In some extant species sexual zygotes may also encyst and form a resting hypnozygote. Hypnozygotes are morphologically and developmentally undistinguishable from the vegetative stomatocysts of the same species (Sandgren 1988). Only a small number of extant freshwater stomatocysts can be attributed to their vegetative cells, but they are species-specific when fully developed (Kristiansen and Andersen 1986; Duff et al. 1995; Holen 2014). Because the current systematics of living freshwater chrysophytes is based on their dominant vegetative stages, the taxonomy of the extant freshwater stomatocysts that have not been attributed to their living stages is also artificial. Newly recognised cyst morphotypes are assigned consecutive numbers in the author's record of cyst descriptions (e.g., Statospore No. 1 Cronberg in Cronberg and Sandgren 1986). Following the proposal of Cronberg and Sandgren (1986), hundreds of such numbered freshwater entities have been described by many authors (Wilkinson et al. 2001; Firsova et al. 2012; Piątek 2017) as an alternative to the equally artificial Linnaean system established by Deflandre (1932c) for fossil marine forms. Attempts have been made to standardise descriptions and recognition of cyst morphotypes (reviewed by Cronberg 1986), but both systems remain in use (compare Wilkinson et al. 2001; Riaux-Gobin and Stumm 2006; Kato 2019). Here, we follow the Deflandre (1932c) system.

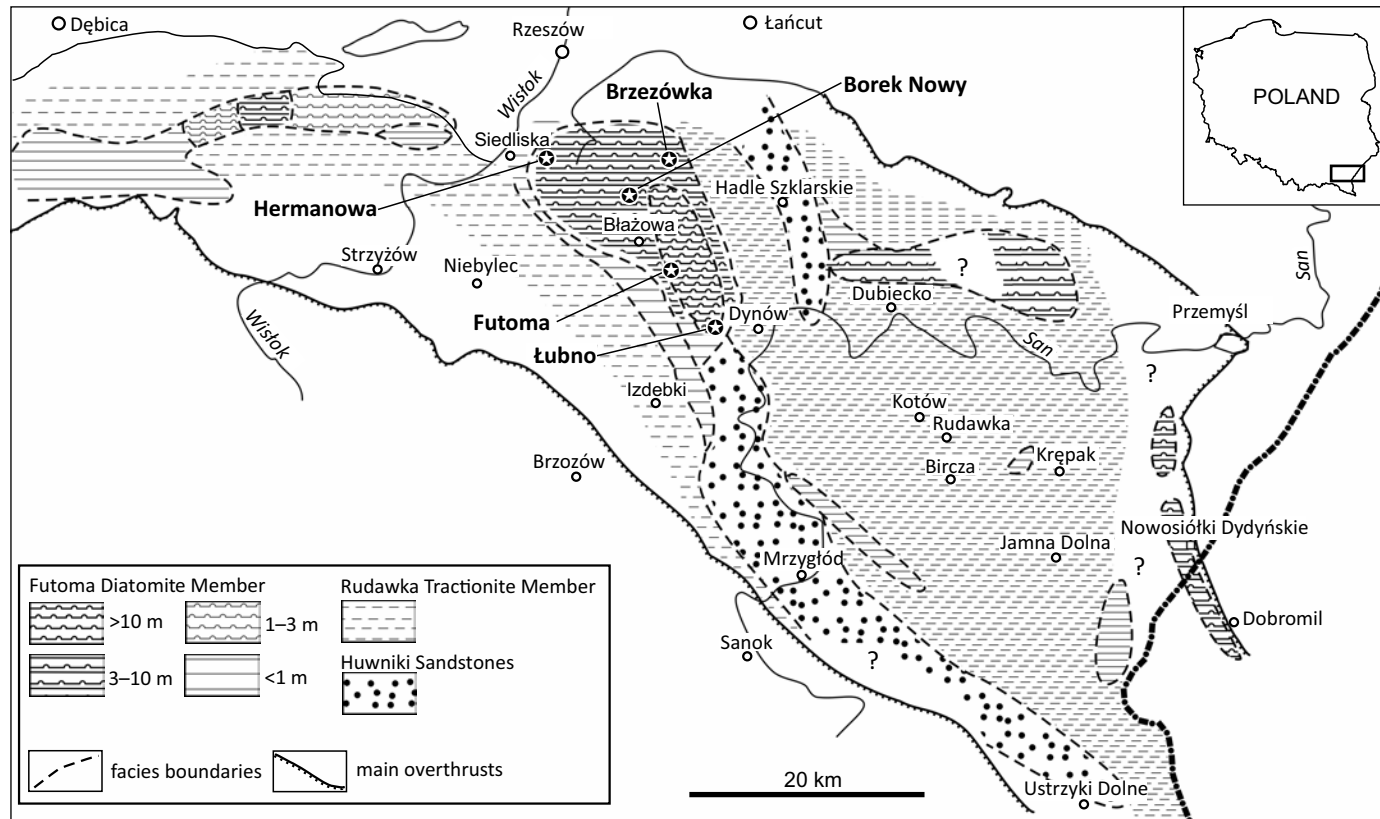


Fig. 1. Lithofacial map of the Menilite Formation below sheet-like shales complex (Borek Nowy member). Redrawn and modified from Kotlarczyk and Leśniak (1990, fig. 7), with permission of AGH University of Krakow Publishing, 2025.

Siliceous scales covering flagellated microeukaryote vegetative cells are minute and relatively lightly silicified when compared to stomatocyst walls (Bessudova et al. 2018; Siver 2020). As such, they are more susceptible to recycling after cell death, during sedimentation, and diagenesis. This at least in part must contribute to their rarity among many relatively well-preserved siliceous fossil-rich sediments. Compared to the number of described stomatocysts, the full set of vegetative cell body-scales have been documented only in relatively few living freshwater chrysophyceans. There is a singular such case among the fossilised freshwater taxa (Siver 2020), and none yet reported among marine taxa (Riaux-Gobin and Stumm 2006). Stomatocysts therefore are and will likely remain into the foreseeable future, the main available evidence of chrysophycean existence in both marine and freshwater fossil records.

We document here for the first time Oligocene archaeomonad stomatocyst flora from the Central Paratethys, Outer Carpathians. When possible, we place all in their Rupelian palaeoenvironmental and micropalaeontological contexts.

*Nomenclatural acts.*—This published work and the nomenclatural acts it contains, have been registered in Phycobank ID: <http://phycobank.org/105035-42>.

*Institutional abbreviations.*—AGH, Academy of Mining and Metallurgy, Kraków, Poland; B, Botanischer Garten und Botanisches Museum, Berlin, Germany; DMF, Digital Microscopy Facility, Mount Allison University, Sackville, Canada; GITAM, Gandhi Institute of Technology and Management, Rushikonda, India; Herbarium KRAM, Herbarium Instituti Botanici, Academiae Scientorum Poloniae-Cracoviae, Kraków, Poland; KRAM, W. Szafer Institute of Botany, Polish Academy of Sciences, Kraków, Poland; NSERC, Natural Sciences and Engineering Research Council of Canada; PAS, Polish Academy of Sciences.

*Other abbreviations.*—LM, light microscopy; ICN, International Code of Nomenclature for algae, fungi, and plants; SEM, scanning electron microscopy.

## Material and methods

Sampling was conducted in southeastern Poland at all sites meeting the criteria indicated in Kotlarczyk and Kaczmarska (1987) and Kaczmarska and Ehrman (2023), i.e., diatom remains detected using field LM or when siliceous microfossils were expected from the position in lithographic succession. A map with sampling sites and illustrating the distribution of the Futoma Diatomite Member and some other contemporary lithofacies is given in Fig. 1. In total, 265 field samples collected in the 1970s were re-examined in the laboratory for the presence of fossilised siliceous remains using LM water mounts, and 123 of them contained identifiable fragments of diatoms.

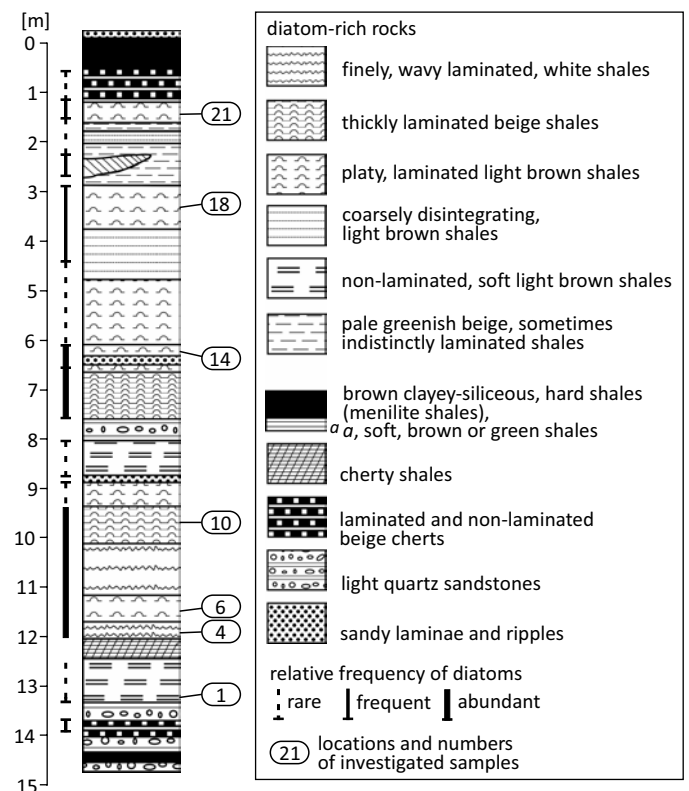


Fig. 2. Lithological columns of Futoma Diatomite Member at its stratotype in Futoma. Redrawn and modified from Kotlarczyk and Kaczmarska (1987, fig. 3), with permission of Annales Societatus Geologorum Poloniae, 2025.

In the Futoma Diatomite Horizon (Kotlarczyk 1982), later named Futoma Diatomite Member (Kotlarczyk et al. 2006), 74 of the 123 samples were found to contain a sufficient quantity of well-preserved siliceous remains to warrant in-depth examination. In this initial report we focus on 17 samples with the most diverse and best preserved archaeomonads and nannofossils collected from outcrops near the villages of Borek Nowy, Brzezówka, Futoma, Hermanowa, and Łubno (Fig. 1). Sedimentary features of the Futoma Diatomite Member of the stratotype at Futoma are shown in Fig. 2. The geological setting for the area and these samples is described in Kotlarczyk and Kaczmarska (1987) and Kotlarczyk and Leśniak (1990).

Sample selection and laboratory processing methods are described in Kaczmarska (1982), Kotlarczyk and Kaczmarska (1987) and Kaczmarska and Ehrman (2023). More recently updated and integrated stratigraphy and palaeoecology of the lower Oligocene (Rupelian) of the sampled area may be found in Kotlarczyk et al. (2006) and Kotlarczyk and Uchman (2012). Alternative palaeoceanographic scenarios are discussed in Sachsenhofer et al. (2017) and Salata and Uchman (2019). SEM examination was performed using a Hitachi SU3500 SEM (Hitachi High-Technologies Canada, Inc., Etobicoke, Ontario, Canada) operating at 10 kV and 5 mm working distance as described in Kaczmarska and Ehrman (2023).

Table 1. Epoch-level range of occurrence for previously described archaeomonad species found in this study. Sources: 1, Bachmann 1964; 2, Buck and Garrison 1983; 3, Cornell 1972; 4, Deflandre 1932a; 5, Deflandre 1933; 6, Deflandre 1938; 7, Deflandre and Deflandre-Rigaud 1969; 8, Gombos 1977; 9, Hajós 1968; 10, Hajós and Stradner 1975; 11, Kato 2019; 12, Ling and Kim 1983; 13, Mitchell and Silver 1982; 14, Mitchell and Silver 1986; 15, Perch-Nielsen 1975; 16, Perch-Nielsen 1978; 17, Rampi 1940; 18, Rampi 1969; 19, Riaux-Gobin and Stumm 2006; 20, Riaux-Gobin et al. 2011; 21, Stradner 1971; 22, Takahashi et al. 1986; 23, Tynan 1960.

| Species name                                   | Upper Cretaceous | Paleocene | Eocene | Oligocene | Miocene | Pliocene | Pleistocene | Recent | Sources                          |
|--|------------------|-----------|--------|-----------|---------|----------|-------------|--------|----------------------------------|
| <i>Archaeomonas chiarugii</i>                  | ×                |           |        |           |         |          |             |        | 10, 17                           |
| <i>Archaeomonas simplicia</i>                  | ×                |           | ×      |           |         |          |             |        | 15, 16, 17, 18                   |
| <i>Archaeomonas kreyenhausenensis</i>          | ×                |           | ×      |           |         |          |             |        | 15, 16, 18                       |
| <i>Archaeomonas robusta</i>                    |                  |           | ×      |           |         |          |             |        | 16, 18                           |
| <i>Archaeomonas karinae</i>                    |                  |           | ×      |           |         |          |             |        | 16                               |
| <i>Archaeomonas americana</i>                  |                  |           | ×      |           |         |          |             |        | 15, 18                           |
| <i>Archaeosphaeridium australensis</i>         |                  |           | ×      | ×         |         |          |             |        | 8, 15                            |
| <i>Litheusphaerella spectabilis</i>            | ×                | ×         | ×      |           | ×       |          |             | ×      | 4, 7, 13, 14, 15, 16, 21, 22     |
| <i>Archaeomonas heteroptera</i>                | ×                | ×         | ×      |           | ×       |          |             |        | 1, 3, 7, 10, 15, 17, 18          |
| <i>Archaeomonas manginii</i>                   | ×                |           | ×      |           | ×       |          |             |        | 1, 3, 4, 9, 15, 17, 18, 21, 23   |
| <i>Archaeomonas helminthophora</i>             | ×                | ×         | ×      |           | ×       |          |             |        | 3, 5, 9, 16, 23                  |
| <i>Archaeomonas vermiculosa</i>                | ×                | ×         | ×      |           | ×       |          |             |        | 3, 4, 16, 17, 21, 23             |
| <i>Archaeomonas speciosa</i>                   | ×                |           |        |           | ×       |          |             |        | 3, 4, 16, 23                     |
| <i>Archaeomonas sphaerica</i>                  |                  | ×         | ×      |           | ×       |          |             |        | 4, 9, 16                         |
| <i>Archaeomonas striata</i>                    |                  | ×         | ×      |           | ×       |          |             |        | 5, 15, 16                        |
| <i>Archaeomonas gratiosa</i>                   |                  |           |        |           | ×       |          |             |        | 9                                |
| <i>Archaeomonas hungarica</i>                  |                  |           |        |           | ×       |          |             |        | 9                                |
| <i>Archaeomonas reticulata</i>                 |                  |           |        |           | ×       |          |             |        | 9                                |
| <i>Archaeomonas ovoidea</i>                    |                  |           |        |           | ×       |          |             |        | 5, 7, 16                         |
| <i>Archaeomonas tubulata</i>                   |                  |           |        |           | ×       |          |             |        | 6, 7                             |
| <i>Archaeomonas mamilliosa</i>                 |                  |           |        |           | ×       |          |             |        | 1, 12, 23                        |
| <i>Archaeomonas japonica</i>                   |                  |           | ×      | ×         | ×       | ×        |             |        | 5, 15, 16, 18                    |
| <i>Archaeomonas areolata</i>                   |                  |           |        |           | ×       | ×        |             | ×      | 2, 5, 11, 13, 14, 16, 21, 22, 23 |
| <i>Archaeomonas</i> cf. <i>areolata</i> var. 1 |                  |           |        |           |         |          |             | ×      | 19, 20                           |

We follow Deflandre's description and naming system (Deflandre and Deflandre-Rigaud 1969) which is commonly used for stomatocysts recovered from marine sediments (Hajós 1968; Perch-Nielsen 1978) and is similar to the conventions for other marine microfossil morphospecies (e.g., acritarchs, coccolithophorids) that use binomial nomenclature notwithstanding their unknown relationship to the entire organism from which they originated. Whenever appropriate, we follow the terminology for stomatocyst structure proposed by Wilkinson et al. (2001) and Kato (2019). Our measurements represent the longest structures on the preserved fossil surfaces. Stratigraphic distribution of previously described species is reported in Table 1.

As some of our SEM preparations are still being investigated for other taxa, permanent repository numbers are not available and instead are identified by provisional DMF numbers. KRAM has agreed to accept these preparations when work is finished and will assign them KRAM numbers when deposited.

## Systematic palaeontology

Division, class, and order uncertain

Family Archaeomonadaceae Deflandre, 1932c

Genus *Archaeomonas* Deflandre, 1932c

*Type species: Archaeomonas manginii* Deflandre, 1932a. Upper Cretaceous–Miocene, California (USA).

*Archaeomonas* stomatocysts with ribs

*Archaeomonas lenistriata* Kaczmarek sp. nov.

Fig. 3A–F.

*PhycoBank ID:* <http://phycobank.org/105035>.

*Etymology:* Refers to delicate ribbing of the cyst walls.

*Holotype:* DMF SEM stub 349-2, as preparation KRAM A-28, sample Borek Nowy Kawalec (Fig. 3A, SEM image of fractured stomatocyst in antero-lateral view).

*Type locality:* Borek Nowy Kawalec, Poland.



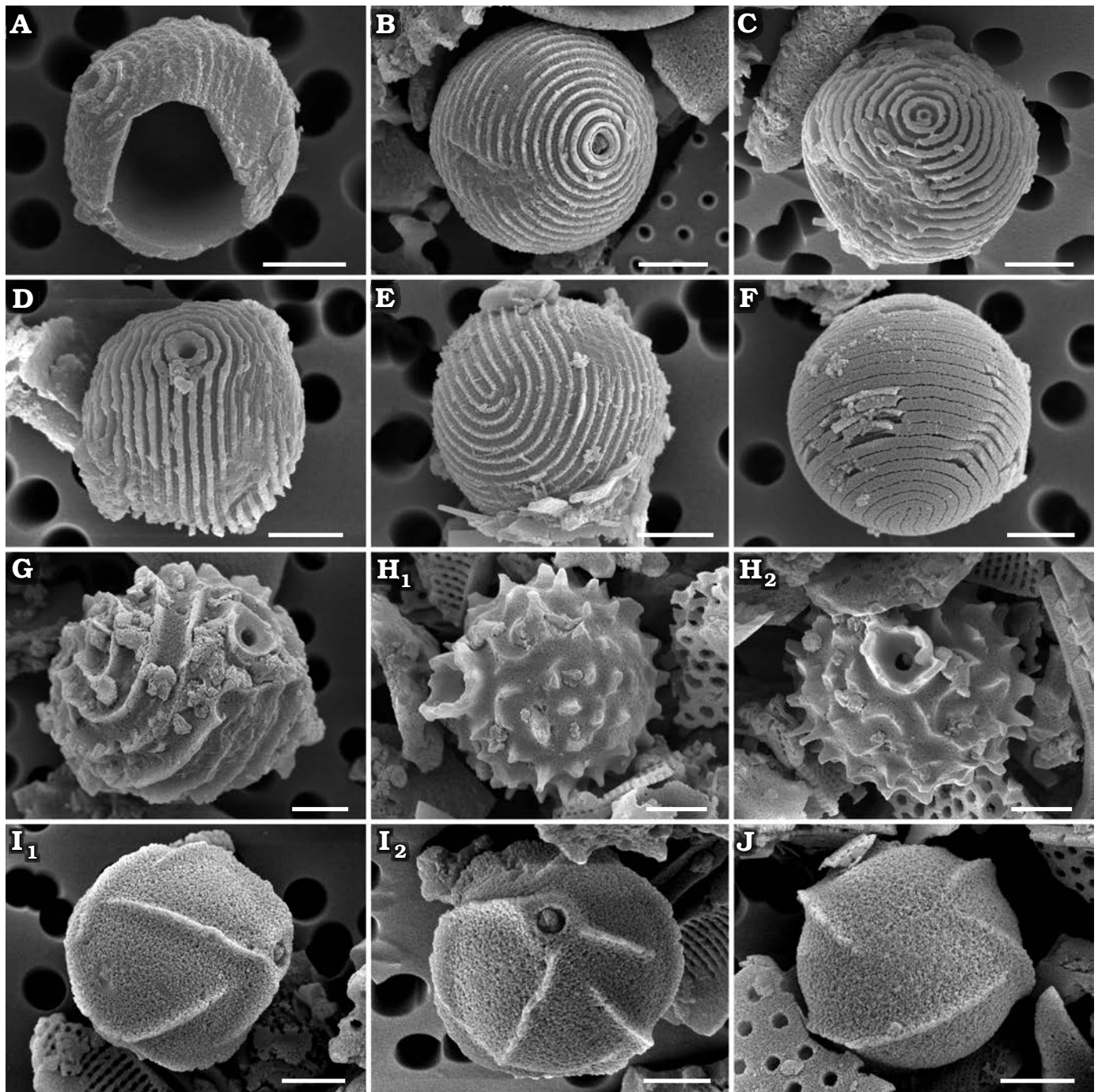


Fig. 3. Archaeomonad stomatocysts from Rupelian (lower Oligocene) of Poland. **A–F.** *Archaeomonas lenistriata* Kaczmarek sp. nov., variant with concentric orientation of strips (**A–C**), variant with strips looping around anterior and posterior poles (**D–F**). **A.** DMF stub 349-2 (KRAM A-28), holotype, Borek Nowy Kawalec, in antero-lateral view. **B.** DMF stub 333-3, Brzezówka, in antero-lateral view. **C.** DMF stub 349-2 (KRAM A-28), Borek Nowy Kawalec, in antero-lateral view. **D.** DMF stub 349-2 (KRAM A-28), Borek Nowy Kawalec, in antero-lateral view. **E.** DMF stub 349-2 (KRAM A-28), Borek Nowy Kawalec, in postero-lateral view. **F.** DMF stub 349-2 (KRAM A-28), Borek Nowy Kawalec, in postero-lateral view. **G.** *Archaeomonas striata* Deflandre, 1933, DMF stub 349-17a, Futoma 4, in antero-lateral view. **H.** *Archaeomonas genetyanii* Ehrman sp. nov., DMF stub 349-16 (KRAM A-30), Futoma 4, holotype, in lateral view (**H<sub>1</sub>**), anterior view showing details of collar and pore (**H<sub>2</sub>**). **I, J** *Archaeomonas gratiosa* Hajós, 1968, Futoma 5. **I.** DMF stub 352-1a, stomatocyst, in antero-lateral view (**I<sub>1</sub>**), anterior view showing details of collar and pore (**I<sub>2</sub>**). **J.** DMF stub 352-1b, in posterior view. Scale bars 2  $\mu$ m.

*Type horizon:* Futoma Diatomite Member, Rupelian, lower Oligocene.

*Material.*—Stomatocysts with parallel ribs: Borek Nowy Kawalec (DMF stubs 349-2 as KRAM A-28, 349-2a, 349-2b, 349-2c, 349-2d), Futoma 14. Concentric-ring morphol-

ogy: Borek Nowy Kawalec, Brzezówka (DMF stub 333-3). At least a dozen specimens of each morphology found on SEM stubs (~20 images acquired). All from Oligocene of southeastern Poland.

**Diagnosis.**—Cell walls finely ribbed (may be called striae or ridges, approximately 25–35 in 10  $\mu\text{m}$ ) in pattern parallel to cell apical axis or showing a combination of perpendicular and parallel orientation. Collar in form of low cylinder topped with flat rim.

**Description.**—Stomatocysts spherical, 5.3–8.2  $\mu\text{m}$  in diameter, cell walls with very fine and low ribs (Fig. 3A, B, D, E). Two variants of striation found: perpendicular (Fig. 3A–C) and parallel (Fig. 3D–F) to cyst apical axis (the axis connecting anterior with posterior poles of cyst). In parallel variant ribs loop around collar and descend toward posterior pole where they turn on themselves (Fig. 3D, E). In second variant ribs organised concentrically around collar and parallel to each other but perpendicular to apical axis (Fig. 3B, C). Both morphotypes of similar cell and pore size. Pores surrounded by simple cylindrical, low collar, similar in width and appearance to ribs on cyst surface, collar 0.6–0.7  $\mu\text{m}$  in diameter. Ribs fine, 25–35 in 10  $\mu\text{m}$ . Individual ribs up to 0.3  $\mu\text{m}$  high and abaxially T-shaped when seen on best preserved specimens (Fig. 3C, D, F). In those specimens, rib tops nearly touch each other. In partially eroded specimens only vertical portion of “T” is preserved and so ribs appear further apart, most commonly separated by approximately 0.2  $\mu\text{m}$ .

**Remarks.**—The overall wall general surface architecture of our specimens is similar to *Archaeomonas striata* Deflandre, 1933, discussed below. Ribs looping around the collar and turning on themselves in the parallel variant are also shown in SEM images in Deflandre and Deflandre-Rigaud (1969) where they were erroneously attributed to *A. striata*. However, the rib density is much finer on the walls of *A. lenistriata* Kaczmarek sp. nov. than on the *A. striata* holotype or freshwater Stomatocyst 97 Duff & Smol, 1991. Furthermore, the collars of our specimens are different from those seen on LM and SEM images of the holotype and other specimens of *A. striata* shown by Deflandre (1933) and Perch-Nielsen (1978), leading us to conclude that our specimens represent a species new to science.

**Stratigraphic and geographic range.**—Rupelian (lower Oligocene) of southeastern Poland (this study).

### *Archaeomonas striata* Deflandre, 1933

Fig. 3G.

**Material.**—Six specimens from Futoma 4 (DMF stub 349-17a), Oligocene of southeastern Poland.

**Description.**—Stomatocysts spherical, 9–10  $\mu\text{m}$  in diameter. Cell wall ornamented by narrow, tall ribs (up to 0.6  $\mu\text{m}$  tall; 7–8 ribs in 10  $\mu\text{m}$ ) separated by wide depressions. Depending on cyst orientation, ribs may appear spiral, looping or nearly longitudinal between cyst anterior and posterior poles. Pores regular, 0.7  $\mu\text{m}$  in diameter surrounded by a collar with obconical, concave flange, 2.2  $\mu\text{m}$  in maximal diameter (Fig. 3G).

**Remarks.**—*Archaeomonas striata* (Deflandre 1933; Deflandre and Deflandre-Rigaud 1969) from Jutland (Denmark)

is the most similar to our specimens. Although several specimens are shown in those sources, just one measurement is given which is for the cyst diameter (5.5  $\mu\text{m}$ ). The species is also reported by Perch-Nielsen (1978) and on those cysts the ribs (there called striae) also loop and split in the manner illustrated by Deflandre (1933). Her specimens are also coarsely striated (~9 in 10  $\mu\text{m}$ ), similar to the LM-documented holotype shown by Deflandre (1933) with 5–7 striae on the visible side of the spherical cell when counted on her images. Freshwater Stomatocyst 97 Duff & Smol, 1991, is somewhat similar to our specimens and those of Deflandre (1933) and Perch-Nielsen (1978) in terms of striation density (striae are called circuli in Duff and Smol 1991) but differs in collar structure; conical with ridges continuing onto the collar in Perch-Nielsen (1978) vs. cylindrical, separate and circular in Duff and Smol (1991). Furthermore, there are two SEM images shown by Deflandre and Deflandre-Rigaud (1969) attributed to this species. However, these images carry finer ribbing. At least 13 ribs can be counted on a part of the clearly visible side of the spherical cell while 5–9 is seen on the holotype in Deflandre (1933) and Perch-Nielsen (1978) specimens. Admittedly, any metrics are difficult to establish when only magnifications and not scale bars are provided. Nonetheless, because of the significant difference in rib density between their LM and SEM images, we consider the two specimens illustrated in SEM as belonging to a species other than *A. striata* sensu Deflandre (1933), most likely to our new species *A. lenistriata* Kaczmarek sp. nov.

**Stratigraphic and geographic range.**—Paleocene–Eocene of Mors Island, Denmark (Deflandre 1933), Upper Eocene of the Vøring Plateau of the Norwegian Sea (Perch-Nielsen 1978), Rupelian (lower Oligocene) of southeastern Poland (this study), and Miocene of the Subantarctic Southwest Pacific (Perch-Nielsen 1975).

### *Archaeomonas stomatocysts with ridged walls*

#### *Archaeomonas genetynanii* Ehrman sp. nov.

Fig. 3H.

**Phycobank ID:** <http://phycobank.org/105036>.

**Etymology:** Dedicated to Eugene J. Tynan (1924–1986), who reported extensively on many microfossils including archaeomonads.

**Holotype:** DMF SEM stub 349-16, as preparation KRAM A-30, sample Futoma 4, fine fraction (Fig. 3H<sub>1</sub>, SEM image of stomatocyst in antero-lateral view).

**Type locality:** Futoma, Poland.

**Type horizon:** Futoma Diatomite Member, Rupelian, lower Oligocene.

**Material.**—Several specimens encountered on each SEM stub from Futoma 4 (DMF stub 349-16 as KRAM A-30), 5, Oligocene of southeastern Poland.

**Diagnosis.**—High obconical, concave collar, cyst wall covered with short, curved ridges and prickly spines.

**Description.**—Stomatocysts spherical, 7.4–8.8  $\mu\text{m}$  in diameter. Pores regular, 0.6  $\mu\text{m}$  in diameter surrounded by obconical, concave collar (Fig. 3H<sub>1</sub>) abruptly emerging from



cyst wall surface, up to 0.8  $\mu\text{m}$  high and 2.9  $\mu\text{m}$  in diameter at its irregular free margin. Cyst walls ornamented with short, ridges and prickly spines dispersed throughout (Fig. 3H). Some spines rounded, others polygonal at base. Some ridges straight, others bowed and/or branching. Spines and ridges up to 1.2  $\mu\text{m}$  high, 6–8 in 10  $\mu\text{m}$ .

**Remarks.**—Tynan described and illustrated specimens named “*Archaeomonas cf. helminthophora*” (Tynan 1960). He emphasised significant differences in collar structure between *A. helminthophora* Deflandre, 1933, and his specimens as distinguishing characters between the two. His specimens have a collar distinctly obconical (which he called “flared”), while the holotype of *A. helminthophora* has a low, more cylindrical collar (Deflandre 1933). Unfortunately, in the same publication Deflandre also diagnosed *A. helminthophora* cysts as having “the structure of the pore very low and flared”, contradicting his own drawing of the holotype. The low “flaring” is clearly seen on our specimens; therefore, we attribute them to *A. helminthophora*. Other characteristics of *A. helminthophora* are detailed below. The most immediately notable difference between our new species and the type specimen shown by Deflandre (1933) for *A. helminthophora* is the wall ornamentation. *A. helminthophora* cyst walls carry long ridges while our specimens and those of Tynan (1960) have a mixture of short ridges and various prickly spines.

**Stratigraphic and geographic range.**—Rupelian (lower Oligocene) of southeastern Poland (this study).

#### *Archaeomonas gratiosa* Hajós, 1968

Fig. 3I, J.

**Material.**—Numerous specimens found on each SEM stub from Futoma 5 (DMF stubs 352-1a, 352-1b), Łubno 3, Oligocene of southeastern Poland.

**Description.**—Stomatocysts spherical, 6.0–9.0  $\mu\text{m}$ , pores 0.5–0.9  $\mu\text{m}$  in diameter. Collars indistinct, low, flat-rimmed and cylindrical, 0.8–1.8  $\mu\text{m}$  in diameter (Fig. 3I<sub>1</sub>). Walls ornamented by sparse, thin, sharp ridges, up to 1.1  $\mu\text{m}$  high in best preserved specimens. There may be 2–9 visible ridges, depending on cell orientation (Fig. 3I<sub>2</sub>), but most are distant from each other at 2–4 in 10  $\mu\text{m}$ . Some ridges straight, running parallel to each other over a large part of the cyst surface, others shorter and slightly curved. Ridges may be positioned obliquely, spirally, or radially relative to cyst anterior-posterior axis (Fig. 3J).

**Remarks.**—Our specimens are similar to *A. gratiosa* with its relatively narrow cylindrical collar and ridges “not converging and connecting like in *A. lefeburei* Deflandre, 1933”, which Hajós (1968) deemed its closest relative. However, our specimens are somewhat smaller than those from the Tortonian in Hungary, being just at and below the lower range of the diagnostic size range (8–10  $\mu\text{m}$  in diameter). Other similar species include *A. venusta* Deflandre, 1933 (Deflandre 1933), and *A. gracilis* Tynan, 1960 (Tynan 1960),

but they have pronounced and obconical collars in addition to different patterns of ridges. In *Archaeomonas chenevierei* Deflandre, 1932d (Deflandre 1932d), *A. deflandrei* Rampi, 1948 (Rampi 1948), and *A. lefeburei* (Deflandre 1933) ridges are wavy, joining and branching, unlike our cysts with singular ridges. *A. deflandriana* Hajós, 1968, has an exceptionally long collar and very tall ridges.

**Stratigraphic and geographic range.**—Rupelian (lower Oligocene) of southeastern Poland (this study), and Tortonian (Miocene) of Hungary (Hajós 1968).

#### *Archaeomonas helminthophora* Deflandre, 1933

Fig. 4A, B.

**Material.**—At least 10 specimens encountered on both SEM stubs from Borek Nowy Kawalec (DMF stub 349-2e), Futoma 17 (DMF stub 349-12a), Oligocene of southeastern Poland.

**Description.**—Stomatocysts spherical, 6.6–7.1  $\mu\text{m}$  with pores 0.6  $\mu\text{m}$  in diameter. Pores surrounded by low, cylindrical to obconical collars, up to 2.6  $\mu\text{m}$  in diameter (Fig. 4A). Cyst walls adorned with high, narrow ridges of varied length and orientation, both straight and slightly bowed (Fig. 4B) but generally equal to or longer than collar diameter, as shown on the species holotype. As per diagnosis, number of ridges varies greatly. Maximal height of undamaged ridge recovered was 1.6  $\mu\text{m}$ .

**Stratigraphic and geographic range.**—Upper Cretaceous of the Moreno Formation, California (USA; Cornell 1972), Rupelian (lower Oligocene) of southeastern Poland (this study), Miocene of Maryland (USA; Deflandre 1933; Tynan 1960), Tortonian (Miocene) of Hungary (Hajós 1968; Deflandre and Deflandre-Rigaud 1969), and Miocene of the Vøring Plateau of the Norwegian Sea (Perch-Nielsen 1978).

#### *Archaeomonas heteroptera* Deflandre, 1932c

Fig. 4C–E.

**Material.**—Numerous specimens encountered on each SEM stub from Borek Nowy 12 Kawalec, Futoma 5, 17 (DMF stub 349-12b), Łubno 3 (DMF stub 342-10a), 4 (DMF stub 333-10a), Oligocene of southeastern Poland.

**Description.**—Stomatocysts appear spherical, oblate, or ellipsoidal, depending on cell orientation; 6.0–8.8  $\mu\text{m}$  and 6.2–9.5  $\mu\text{m}$  in width and length, respectively. Pores 0.6–1.2  $\mu\text{m}$  in diameter, surrounded by cylindrical collar (Fig. 4C) with relatively thick flat rim (Fig. 4D). Collars 1.3–2.7  $\mu\text{m}$  in diameter including rim and up to 0.8  $\mu\text{m}$  high in best preserved specimens. Cyst walls adorned with tall, fin-like longitudinal ridges. Several longest ridges may run nearly entire length of cell (Fig. 4C), while shorter ridges may be inserted between longer ones. Number and length of ridges varies greatly (Fig. 4E). Maximal height of ridge recovered was 1.5  $\mu\text{m}$ . There may be 2–8 such ridges in 10  $\mu\text{m}$ . State of specimen preservation varied, some showing only bases of ridges (Fig. 4D). In extreme cases, although generally

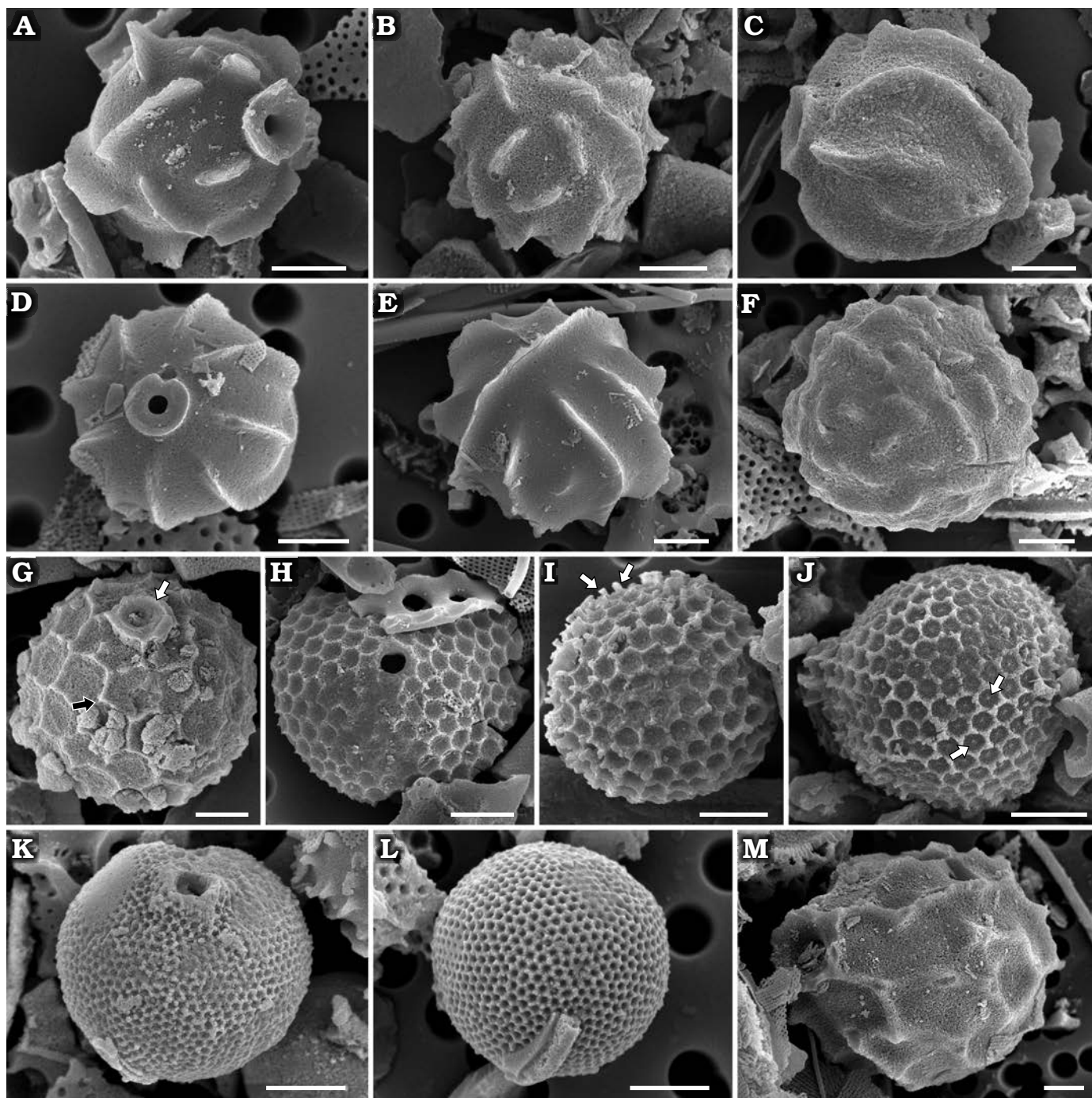


Fig. 4. Archaeomonad stomatocysts from Rupelian (lower Oligocene) of Poland. **A, B.** *Archaeomonas helminthophora* Deflandre, 1933. **A.** DMF stub 349-2e, Borek Nowy Kawalec, in antero-lateral view. **B.** DMF stub 349-12a, Futoma 17, in posterior view. **C–E.** *Archaeomonas heteroptera* Deflandre, 1932c. **C.** DMF stub 349-12b, Futoma 17, in lateral view. **D.** DMF stub 342-10a, Lubno 3, in anterior view. **E.** DMF stub 333-10a, Lubno 4, in posterior view. **F.** *Archaeomonas vermiculosa* Deflandre 1932a, DMF stub 349-12c, Futoma 17, in lateral view. **G.** *Archaeomonas areolata* Deflandre, 1933, DMF stub 349-17b, Futoma 4, in antero-lateral view, with thick, internally round externally polygonal ring of a collar (white arrow) with conulae at some junctions of polygons on wall surface (black arrow). **H–J.** *Archaeomonas* cf. *areolata* var. 1 Riaux-Gobin & Stumm, 2006. **H.** DMF stub 341-13, Lubno 4, in anterior view. **I.** DMF stub 342-15a, Borek Nowy 12B, in posterior view, with blunt, bacculate spines at neighboring polygon junctions (arrows). **J.** DMF stub 349-1, Futoma 17A, in lateral view, with small conulae visible in areolae centers (arrows). **K, L.** *Archaeomonas asharya* Samanta sp. nov. **K.** DMF stub 349-12 (KRAM A-29), holotype, Futoma 17, in antero-lateral view. **L.** DMF stub 333-5, Futoma 17A, in posterior view. **M.** *Archaeomonas ovoidea* Deflandre, 1933, DMF stub 342-13 (B 40 0046308), Lubno 4, in lateral view. Scale bars 2  $\mu$ m.

spherical, overall cyst outline appeared angular. In such cysts, the pores have acute edges, flush with surrounding flattened cell surface and no collar.

**Remarks.**—In addition to Deflandre (1932a, c) this variable, yet distinct species has been reported by several researchers, as summarised and illustrated in Deflandre and Deflandre-



Rigaud (1969), but also later by Perch-Nielsen (1978), both including SEM images.

*Stratigraphic and geographic range.*—Upper Cretaceous of the Moreno Formation, California (USA; Rampi 1940; Cornell 1972), Upper Cretaceous of the South Pacific Ocean (Hajós and Stradner 1975), Paleocene/Eocene boundary of Fuur Island, North Jutland (Denmark; Deflandre and Deflandre-Rigaud 1969), Eocene of the Kreyenhagen Formation, California (USA; Rampi 1969), Upper Eocene of the Subantarctic Southwest Pacific (Perch-Nielsen 1975), Rupelian (lower Oligocene) of southeastern Poland (this study), Miocene of the Calvert Formation, Maryland (USA; Tynan 1960), Miocene of Noto Peninsula (Japan; Bachmann 1964), and Miocene of Limberg (Austria; Stradner 1971).

#### *Archaeomonas vermiculosa* Deflandre, 1932a

Fig. 4F.

*Material.*—Several specimens encountered on SEM stub from Futoma 17 (DMF stub 349-12c), Oligocene of southeastern Poland.

*Description.*—Cysts spherical, 6.6–9.2  $\mu\text{m}$  in diameter. Walls densely covered with irregularly dispersed vermicular ribs of varied length, straight or slightly curved (Fig. 4F). Maximal height of ridge recovered was 0.6  $\mu\text{m}$ . One cyst presenting pore shows a relatively small, regular opening, 0.6  $\mu\text{m}$  in diameter. Collar subconical, up to 1.1  $\mu\text{m}$  in diameter and approximately 0.5  $\mu\text{m}$  in height.

*Remarks.*—The subconical collar, smaller and denser ridges distinguish our specimens from those of *A. helminthophora* (Deflandre 1933). Our specimens differ from that shown by Perch-Nielsen (1978) by having a less spinose character of the ribs and are slightly larger than all specimens mentioned above. The ribs on our specimens tend to be longer and more curved towards the posterior end of the cyst, in agreement with the illustration of the holotype.

*Stratigraphic and geographic range.*—Upper Cretaceous of the Moreno Formation, California (USA; Rampi 1940; Cornell 1972), Paleocene/Eocene boundary of Fuur Island, North Jutland (Denmark; Deflandre 1932a), Rupelian (lower Oligocene) of southeastern Poland (this study), Miocene of the Calvert Formation, Maryland (USA; Tynan 1960), Miocene of Limberg (Austria; Stradner 1971), and Miocene of the Vøring Plateau of the Norwegian Sea (Perch-Nielsen 1978).

#### *Archaeomonas* stomatocysts with reticule

##### *Archaeomonas areolata* Deflandre, 1933

Fig. 4G.

*Material.*—Numerous specimens encountered on each SEM stub from Futoma 4 (DMF stub 349-17b), 5, 17, Oligocene of southeastern Poland.

*Description.*—Spherical specimens 7.7–9.3  $\mu\text{m}$  in diameter. Pores 0.7–0.8  $\mu\text{m}$  in diameter surrounded by thick, internally round, externally polygonal ring of a collar (Fig. 4G)

slightly elevated above cell wall surface and connected to sides of neighbouring polygons, 1.7–2.4  $\mu\text{m}$  in diameter. Cell walls covered by relatively large polygonal (mostly hexagonal) reticulum, 4–7 areolae in 10  $\mu\text{m}$ , sometimes referred to as locunae. Small conulae (up to 0.4  $\mu\text{m}$  high; Fig. 4G) may emerge at junctions of some polygons, as in Deflandre's (1933) holotype.

*Remarks.*—Following the original description, Tynan (1960) and Stradner (1971) provided images of specimens with a very low, simple cylindrical collar. Later, Perch-Nielsen (1978) showed specimens with a varying degree of wall structure erosion. Our specimens are most similar to her's (Perch-Nielsen 1978: pl. 1: 10), with relatively low walls of areolae and simplified collar. Although metrics for the specimens are not given, they generally agree with Deflandre's and Tynan's cyst sizes (6–7  $\mu\text{m}$ ) when calculated from their images (Stradner 1971; Perch-Nielsen 1978). Areolae density of all their specimens is approximately 7–9 areolae in 10  $\mu\text{m}$ , thus similar to ours. Specimens attributed to *A. areolata*, *A. cf. areolata*, *A. cf. areolata* var. 1, and *A. cf. areolata* var. 2 have been found in modern Antarctic waters associated with sea-ice (Mitchell and Silver 1982; Buck and Garrison 1983; Riaux-Gobin and Stumm 2006). The most notable difference between these, our specimens, and fossil *A. areolata* sensu lato is the somewhat greater density of areolae (10–14 in 10  $\mu\text{m}$  in the case of *A. cf. areolata* var. 1) and more variable cyst size and shape, in addition to the finer density wall areolae (6.6–10.0 in 10  $\mu\text{m}$ ) in the case of *A. cf. areolata* var. 2. However, taxonomic affinity to the modern specimens attributed to *A. areolata* requires careful comparison to Deflandre's (1933) type material.

*Stratigraphic and geographic range.*—Rupelian (lower Oligocene) of southeastern Poland (this study), Miocene of the Calvert Formation, Maryland (USA; Tynan 1960), Miocene of Limberg (Austria; Stradner 1971), Miocene of the Vøring Plateau of the Norwegian Sea (Perch-Nielsen 1978), Miocene/Pliocene boundary of Hungary (Deflandre 1933), and Miocene/Pliocene boundary of Atlantic section of Southern Ocean (Kato 2019). Recent reports from the Equatorial Pacific, North Pacific, and South Atlantic (Mitchell and Silver 1982), the Weddell Sea (Buck and Garrison 1983; Mitchell and Silver 1986), and Kita-no-seto Strait, Antarctica (Takahashi et al. 1986).

##### *Archaeomonas cf. areolata* var. 1 Riaux-Gobin & Stumm, 2006

Fig. 4H–J.

*Material.*—Numerous specimens encountered on each SEM stub from Borek Nowy 5, 12B (DMF stub 342-15a), Futoma 5, 17A (DMF stub 349-1), Łubno 4 (DMF stub 341-13), Oligocene of southeastern Poland.

*Description.*—Cells spherical, 6.3–8.1  $\mu\text{m}$  in diameter. External wall surface covered by regular lattice of mostly hexagonal, equally sized areolae, 11–15 in 10  $\mu\text{m}$  (Fig. 4H). In well preserved specimens, blunt, bacculate spines emerge

at junctions of wall between neighbouring polygons, up to 0.6  $\mu\text{m}$  high (Fig. 4I). In still better-preserved specimens, small conulae may be visible in areolae centers (Fig. 4J). Pores 0.5–0.8  $\mu\text{m}$  in diameter surrounded by low collar, 1.4–1.5  $\mu\text{m}$  in diameter (Fig. 4H). Rim surrounding pores are circular internally but polygonal externally and connecting to sides of neighbouring polygons.

**Remarks.**—Among the areolate forms, this stomatocyst is the most common and widely distributed in our samples. The morphologically most similar stomatocyst known is the modern Antarctic *Archaeomonas* cf. *areolata* var. 1 described by Riaux-Gobin and Stumm (2006). Ours and the specimens from Antarctica differ from *A. areolata* by having finer areolae. Cyst Type 3 and 4 VanLandingham, 1964, from Washington state (USA) show a larger range of sizes and density of areolation and altogether are similar (but not identical) to forms reported from the humic Lake Gribso (Nygaard 1956).

### *Archaeomonas asharya* Samanta sp. nov.

Fig. 4K, L.

PhycoBank ID: <http://phycobank.org/105037>.

**Etymology:** Dedicated to my wife and son.

**Holotype:** DMF SEM stub 349-12, as preparation KRAM A-29, sample Futoma 17, intermediate fraction (Fig. 4K, SEM image of stomatocyst in anterio-lateral view).

**Type locality:** Futoma, Poland.

**Type horizon:** Futoma Diatomite Member, Rupelian, lower Oligocene.

**Material.**—Several specimens encountered on each SEM stub from Futoma 5, 17 (DMF stub 349-12 as KRAM A-29), 17A (DMF stub 333-5), Oligocene of southeastern Poland.

**Diagnosis.**—Cysts with conical collars and hexagonal lattice on external sides.

**Description.**—Stomatocysts spherical, 5.8–6.4  $\mu\text{m}$  in diameter. Collars conical, topped with flat rounded rims, up to 0.8  $\mu\text{m}$  high, up to 2.2  $\mu\text{m}$  in basal diameter and 1.2  $\mu\text{m}$  at rims. Pores regular, approximately 0.8  $\mu\text{m}$  in diameter. Cyst walls including collar external sides covered with hexagonal lattice of regularly organised scabra, 29–34 hexagons in 10  $\mu\text{m}$  (Fig. 4K). Lattice often organised into areas with parallel or fasciculate rows of areolae (Fig. 4L).

**Remarks.**—Our specimens are somewhat similar to freshwater Stomatocyst 178 Zeeb & Smol, 1993, illustrated in Duff et al. (1995) in the type of wall ornamentation, but our hexagons are coarser (29–34 vs. 40+ in 10  $\mu\text{m}$ , as calculated from their images). Also, the pore-collar systems differ between the species. In Stomatocyst 178 the collar is cylindrical to obconical, while our specimens consistently have conical collars.

**Stratigraphic and geographic range.**—Rupelian (lower Oligocene) of southeastern Poland (this study).

### *Archaeomonas ovoidea* Deflandre, 1933

Figs. 4M, 5A.

**Material.**—Numerous specimens encountered on each SEM stub from Futoma 5, 16 (DMF stub 349-15), Lubno 4 (DMF stub 342-13 as B 40 0046308), Oligocene of southeastern Poland.

**Description.**—Stomatocysts ovate, 13.4–16.3  $\mu\text{m}$  long and 9.8–12.1  $\mu\text{m}$  wide (Figs. 4M, 5A<sub>1</sub>) with externally short “neck” grading into obconical collar surrounding pores, 1.8  $\mu\text{m}$  in diameter. Collar rim carries short conulae that are also connected to wall ridges (Fig. 5A<sub>2</sub>). Collars 2.9–4.3  $\mu\text{m}$  in apical diameter. Wall surface covered by polygonal network of irregular, low ridges carrying minute scabra or conulae mostly at ridge junctions and rims of collars, 2–7 ridges in 10  $\mu\text{m}$ , most commonly only 3 in 10  $\mu\text{m}$ .

**Remarks.**—This species is infrequently reported. In addition to the holotype, the species and a similar form (*A. cf. ovoidea*) have been found by Perch-Nielsen (1978). Perch-Nielsen’s specimens show more regularity in the network of ridges than described and shown on the holotype.

**Stratigraphic and geographic range.**—Rupelian (lower Oligocene) of southeastern Poland (this study), Middle Miocene of San Pedro, California (USA; Deflandre 1933; Deflandre and Deflandre-Rigaud 1969), and Middle to Upper Miocene of the Vøring Plateau of the Norwegian Sea (Perch-Nielsen 1978).

### *Archaeomonas* stomatocysts with reticule and spines

#### *Archaeomonas* aff. *chiarugii* Rampi, 1940

Fig. 5B.

**Material.**—Several specimens encountered on each SEM stub from Borek Nowy 5B (DMF stub 342-18); Futoma 17, Oligocene of southeastern Poland.

**Description.**—Stomatocysts spherical, 4.8–7.2  $\mu\text{m}$  in diameter. Collar and cyst external surface covered with a reticle of polygons of variable size, 11–30 ribs in 10  $\mu\text{m}$  (Fig. 5B). Sides of polygons vary in thickness. Small spines and conulae most common on the thickest ridges. Pores 0.5–0.7  $\mu\text{m}$  in diameter, surrounded by slightly conical collar with acute rim. Collars 0.7–1.3  $\mu\text{m}$  in diameter.

**Remarks.**—Our specimens are somewhat similar to *A. chiarugii* in their fine reticular sculpturing of the walls. Otherwise, our specimens are smaller, their collars are less offset from the cyst body, and reticulation is less regular.

#### *Archaeomonas hungarica* Hajós, 1968

Fig. 5C–E.

**Material.**—Numerous specimens encountered on each SEM stub from Borek Nowy 5, 12B (DMF stub 342-15b), Futoma 5 (DMF stub 352-2a), 17 (DMF stub 349-12d), Oligocene of southeastern Poland.

**Description.**—Cells spherical, 7.2–8.8  $\mu\text{m}$  in diameter. Pores 0.6–0.9  $\mu\text{m}$  in diameter and surrounded by short, slightly



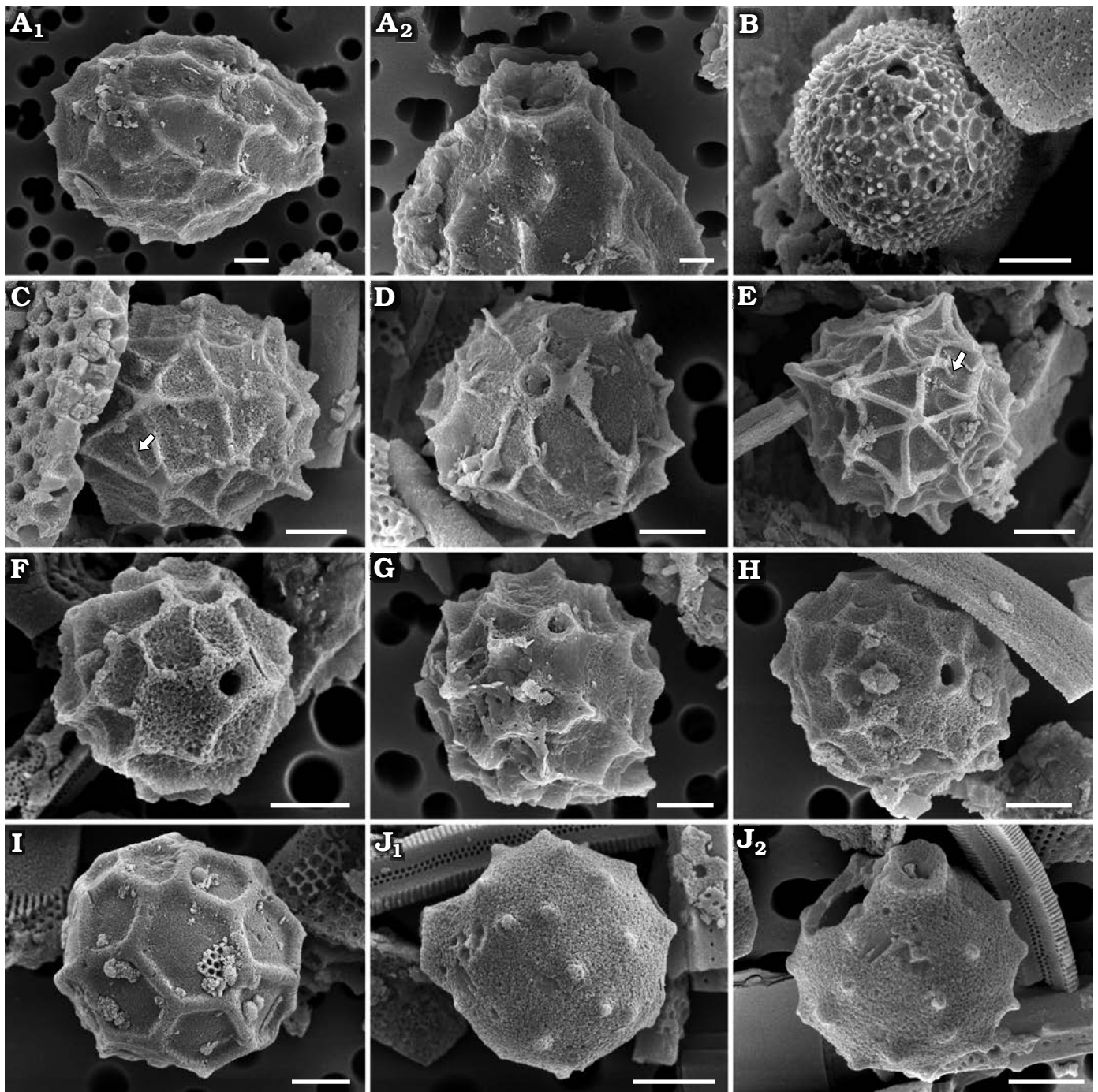


Fig. 5. Archaeomonad stomatocysts from Rupelian (lower Oligocene) of Poland. **A.** *Archaeomonas ovoidea* Deflandre, 1933, DMF stub 349-15, Futoma 16, in lateral view (**A<sub>1</sub>**), antero-lateral view with details of collar and pore (**A<sub>2</sub>**). **B.** *Archaeomonas* aff. *chiarugii* Rampi, 1940, DMF stub 342-18, Borek Nowy 5B, in lateral view. **C–E.** *Archaeomonas hungarica* Hajós, 1968. **C.** DMF stub 352-2a, Futoma 5, in lateral view with tapered ribs inside polygon (arrow). **D.** DMF stub 342-15b, Borek Nowy 12B, in anterior view. **E.** DMF stub 349-12d, Futoma 17, in posterior view, with tapered ribs inside polygon (arrow). **F, G.** *Archaeomonas reticulata* Hajós, 1968 showing variation in wall spination. **F.** DMF stub 352-1c, Futoma 5, in antero-lateral view. **G.** DMF stub 342-9, Borek Nowy 12A, in antero-lateral view. **H.** *Archaeomonas* cf. *reticulata* Hajós, 1968, DMF stub 352-1d, Futoma 5, in antero-lateral view. **I.** *Archaeomonas* cf. *speciosa* Deflandre, 1932a, DMF stub 352-1e, Futoma 5, in posterior view. **J.** *Archaeomonas americana* Rampi, 1969, DMF stub 352-1f, Futoma 5, in lateral view (**J<sub>1</sub>**), antero-lateral view with details of collar and pore (**J<sub>2</sub>**). Scale bars 2  $\mu$ m.

conical collar,  $\sim 0.6$   $\mu$ m high. Collar rim wide, 1.4–2.0  $\mu$ m in diameter (Fig. 5D). In best preserved specimens collar bases connect with ribs covering cyst surface (Fig. 5C, D). Ribs form highly irregular network of polygons, 3–14 polygons

in 10  $\mu$ m. Some ribs taper off before reaching wall of closest opposite polygon (Fig. 5C, E). Conulae and spines may be present at junction of largest polygons or in lacunae of large polygons. Some conulae up to 1.6  $\mu$ m in height.



*Remarks.*—Deflandre and Deflandre-Rigaud (1969) considered *A. hungarica* to be a synonym of *Archaeomonas speciosa* Deflandre, 1932a. Hajós' differential diagnosis (Hajós 1968) emphasizes the collar structure which she considered should be characteristically elevated above the cyst surface in *A. speciosa*. However, such collar elevation is not mentioned in the original description. It is only later shown by Tynan (1960). The original description of *A. hungarica* also emphasises the wall sculpturing. We concur that it is exceptionally varied and as in Hajós' (1968) Tortonian material where among "numerous specimens studied there were no two identical ones". This contrasts to regularly distributed polygons on the holotype and paratypes of *A. speciosa* (Deflandre 1932a; Deflandre and Deflandre-Rigaud 1969, respectively).

*Stratigraphic and geographic range.*—Rupelian (lower Oligocene) of southeastern Poland (this study), and Tortonian (Miocene) of Hungary (Hajós 1968).

#### *Archaeomonas reticulata* Hajós, 1968

Fig. 5F, G.

*Material.*—Several specimens encountered on each SEM stub from Borek Nowy 5, 12A (DMF stub 342-9), Kawalec, Futoma 5 (DMF stub 352-1c), 17, Łubno 4, Oligocene of southeastern Poland.

*Description.*—Stomatocysts spherical, 6.0–10.0  $\mu\text{m}$ , pores 0.7–0.8  $\mu\text{m}$  in diameter. Low and conical collars end in rounded marginal rims. Wall ornamentation consists of net of large, fairly regular polygons, most frequent are tetra- and pentagons, commonly 4–5 in 10  $\mu\text{m}$ , but the entire range is 2–7 in 10  $\mu\text{m}$ . Polygons delineated by ridges. Ridges near collars terminate on collar sides (Fig. 5F). Robust conulae up to 1.0  $\mu\text{m}$  long at junction of several polygons (Fig. 5G). Size of polygons render cyst outline somewhat angular (Fig. 5F).

*Remarks.*—This species has only been reported from the Torton of Hungary (as far as we can determine) where the specimens were somewhat larger (13–14  $\mu\text{m}$ ) than ours. Another species with polygonal cell walls, *A. brevispina* Rampi, 1948, is of similar size but its collar is more strongly developed while spines are more delicate.

*Stratigraphic and geographic range.*—Rupelian (lower Oligocene) of southeastern Poland (this study), and Tortonian (Miocene) of Hungary (Hajós 1968).

#### *Archaeomonas cf. reticulata* Hajós, 1968

Fig. 5H.

*Material.*—Numerous specimens found on each SEM stub from Futoma 5 (DMF stub 352-1d), 17, Oligocene of southeastern Poland.

*Description.*—Stomatocysts spherical, 7.0–8.3  $\mu\text{m}$  in diameter. Pores 0.6–0.9  $\mu\text{m}$  in diameter. Short conical collars end in sharp marginal rims surrounding concave pore (Fig. 5H). Wall ornamentation consists of net of variable polygons, most frequent are tetra- and pentagons, commonly 6–7 in 10  $\mu\text{m}$ , but entire range is 6–15 in 10  $\mu\text{m}$ . Some polygon

ridges terminate on collar sides. Conulae up to 1.0  $\mu\text{m}$  long at junction of ridges.

*Remarks.*—Several specimens found demonstrate general similarity to *A. reticulata* discussed above but carry a finer net of polygons. No intermediate specimens were found. The Late Miocene to Pliocene Stomatocyst 26 Kato, 2019, has similar reticulation, but their pores and collars are unknown due to cyst orientation.

#### *Archaeomonas cf. speciosa* Deflandre, 1932a

Fig. 5I.

*Material.*—Only one specimen from Futoma 5 (DMF stub 352-1e), Oligocene of southeastern Poland.

*Description.*—One stomatocyst found is 8.6–8.8  $\mu\text{m}$  in diameter (Fig. 5I). Cyst wall ornamented with low reticulum and regular, polygonal lacunae, 2.5–3.0 lacunae in 10  $\mu\text{m}$ . Most polygons 5- to 8-sided. Reticulum sides smooth, wide, and up to 0.6  $\mu\text{m}$  high. Small nodules present in junctions of polygon sides. Pore and collar not observed.

*Remarks.*—The size and regular ornamentation of our cyst is most similar to the holotype of *A. speciosa* shown by Deflandre (1932a: fig. 7) which was enlarged in Deflandre and Deflandre-Rigaud (1969). A specimen named "*?Litheusphaerella frenguelli* Defl." in Hajós (1968) may belong to *A. speciosa* as well, as suggested by Deflandre and Deflandre-Rigaud (1969). Stomatocyst 242 Duff & Smol, 1995, reported in Duff et al. (1995) from the freshwater environment is also similar but are about half the size of *A. speciosa* and carry rounded rather than polygonal lacunae. Because the orientation of our specimen does not reveal the pore-collar structure, we consider this identification to be tentative. *A. speciosa* is known from Maryland and California (USA).

#### *Archaeomonas* stomatocysts with spines/nodules

##### *Archaeomonas americana* Rampi, 1969

Fig. 5J.

*Material.*—Numerous specimens encountered on SEM stub Futoma 5 (DMF stub 352-1f), Oligocene of southeastern Poland.

*Description.*—Cysts spherical, 6.0–7.8  $\mu\text{m}$  in diameter. Pores 0.8–0.9  $\mu\text{m}$  in diameter, surrounded by conical collar 1.6–2.3  $\mu\text{m}$  in basal diameter (Fig. 5J<sub>1</sub>). Collar topped by flattened rim surrounding a concave pore (Fig. 5J<sub>2</sub>). Cyst wall surface features sparse, short and stout conulae, generally 3–4 in 10  $\mu\text{m}$ .

*Remarks.*—Our specimens are either slightly smaller or at the lower end of the stomatocyst size range for the species. The somewhat similar *A. cylindropora* Deflandre, 1932a, and *A. manginii* Deflandre, 1932a, differ from our specimens in their collars being cylindrical, both externally and internally and either sparser or denser spines.

*Stratigraphic and geographic name.*—Eocene of the Subantarctic Southwest Pacific (Perch-Nielsen 1975), Eocene

of the Kreyenhagen Formation, California (USA; Rampi 1969), and Rupelian (lower Oligocene) of southeastern Poland (this study).

*Archaeomonas anterioconica* Kaczmarska sp. nov.

Fig. 6A–C.

*PhycoBank ID*: <http://phycobank.org/105038>.

*Etymology*: Refers to conical shape of the anterior pole of the cell.

*Holotype*: DMF SEM stub 333-10, as preparation KRAMA-32, sample Łubno 4 (Fig. 6A, SEM image of stomatocyst in lateral view).

*Type locality*: Łubno, Poland.

*Type horizon*: Futoma Diatomite Member, Rupelian, lower Oligocene.

*Material*.—Numerous specimens encountered on each SEM stub from Borek Nowy 5A (DMF stub 333-4), 12, Kawalec, Brzezówka 32, Hermanowa 27 (DMF stub 342-14), Łubno 4 (DMF stub 333-10 as KRAM A-32), Oligocene of southeastern Poland.

*Diagnosis*.—Cysts subspherical with conical and spineless anterior pole.

*Description*.—Stomatocysts subspherical to ovate with conical anterior pole, 3.0–8.6  $\mu\text{m}$  in diameter. Pores 0.4–0.7  $\mu\text{m}$  in diameter surrounded by conical collar of varying height, 1.1–2.1  $\mu\text{m}$  in diameter and up to 1.1  $\mu\text{m}$  high (Fig. 6A, B). Collar topped by smooth, flat rim (Fig. 6C). Spines irregularly dispersed over most of the cyst surface (0.6–2.3  $\mu\text{m}$  apart), up to 2  $\mu\text{m}$  long near apical pole (Fig. 6A), and about a third of the length at posterior pole, in best preserved specimens (Fig. 6B). A spineless area surrounds collar. Ring of spines pointing towards collar borders area devoid of spines and separate it from spinose part of wall.

*Remarks*.—This is quite a distinct cyst, yet we could not find such specimens in any available report. Although the general distribution of broken spines is reminiscent of *A. manginii*, it differs from it by having a conical anterior pole and spineless area surrounding the collar. Stomatocyst 215 (Duff et al. 1995) is one of the few forms with a similar spineless circum-collar area and they overlap in size with our specimens, but Stomatocyst 215 is spherical, and its collar-pore system is different. Stomatocysts that are morphologically most similar in terms of outline and collar structure are the right-hand SEM images of two cysts shown in Deflandre and Deflandre-Rigaud (1969), named *A. orbicularis* Deflandre, 1933. They however differ in the structure of spines (ours are not elongated at the base), and do not conform to the drawing of the holotype in Deflandre (1933), which lacks the spineless anterior seen on their SEM images.

*Stratigraphic and geographic range*.—Rupelian (lower Oligocene) of southeastern Poland (this study).

*Archaeomonas japonica* Deflandre, 1933

Fig. 6D.

*Material*.—Numerous specimens encountered on each SEM stub from Borek Nowy 12, Futoma 14, Łubno 4 (DMF stub 333-10b), Oligocene of southeastern Poland.

*Description*.—Stomatocysts spherical, 8.0–10.4  $\mu\text{m}$  in diameter. Pores surrounded by cylindrical collar furnished with an uneven rim, collar 1.0  $\mu\text{m}$  high and approximately 2.1  $\mu\text{m}$  in basal diameter (Fig. 6D). Collar height approximately equal to length of robust conulae. Conulae stout, dispersed fairly regularly, up to 1.8  $\mu\text{m}$  long, separated from each other by up to 2  $\mu\text{m}$ . Usually 4–5 bases of conulae visible across cyst equator in lateral view.

*Remarks*.—Our specimens are somewhat larger in diameter than those described by Deflandre (1933; 5.8–6  $\mu\text{m}$ ). The species has also been reported by Rampi (1969) and Perch-Nielsen 1975, 1978), but neither provide metrics. Therefore, our comparisons are based on measurements estimated from their images. Those cyst sizes align our specimens better with *A. oamaruensis* Deflandre, 1933, and *A. cf. japonica* in Perch-Nielsen (1975) than with *A. japonica*. However, the relative proportion of spines and collar height in our specimens meet the criteria for *A. japonica*, while less so for *A. oamaruensis* (Deflandre 1933; Perch-Nielsen 1978), which, in addition, should have a spiny collar. *A. oamaruensis* is reported from New Zealand and the Vøring Plateau of the Norwegian Sea, thus both species were present in Southern and Northern Hemisphere locations of an age similar to our specimens.

*Stratigraphic and geographic range*.—Eocene of the Kreyenhagen Formation, California (USA; Rampi 1969), Upper Eocene of the Vøring Plateau of the Norwegian Sea (Perch-Nielsen 1978), Rupelian (lower Oligocene) of southeastern Poland (this study), upper Oligocene to Miocene of the Subantarctic Southwest Pacific (Perch-Nielsen 1975), and Miocene near Akashiri, Hokkaido (Japan; Deflandre 1933).

*Archaeomonas karinae* Perch-Nielsen, 1978

Fig. 6E–G.

*Material*.—Numerous specimens encountered on each SEM stub from Borek Nowy 5, Futoma 17, Łubno 3, 4 (DMF stubs 333-10c, 333-18a, 333-18b), Oligocene of southeastern Poland.

*Description*.—Cysts spherical, 6.5–9.8  $\mu\text{m}$  in diameter. Pores relatively small, regular, 0.56–0.62  $\mu\text{m}$  in diameter surrounded by externally obconical, internally concave collar (Fig. 6E). Collar 2.1–3.1  $\mu\text{m}$  in diameter with 3–6 small marginal conulae (Fig. 6F). External and internal layers of cyst wall connected by system of cavities when visible in broken specimens. Cyst wall spines robust, up to 2.1  $\mu\text{m}$  long, with flattened tips. Spine sides adorned with longitudinal ribs radiating from base of the spine outwards, some connecting ribbing of neighbouring spines (Fig. 6E, F). Spines regularly dispersed on wall surface, 4–8 in 10  $\mu\text{m}$ .

*Remarks*.—Perch-Nielsen (1978) described this species from the Vøring Plateau of the Norwegian Sea. Although metric data for those specimens are not given, the size estimates from published images (6–8  $\mu\text{m}$  in diameter and robust ribbed spines, 5–6 in 10  $\mu\text{m}$ ) align with the met-



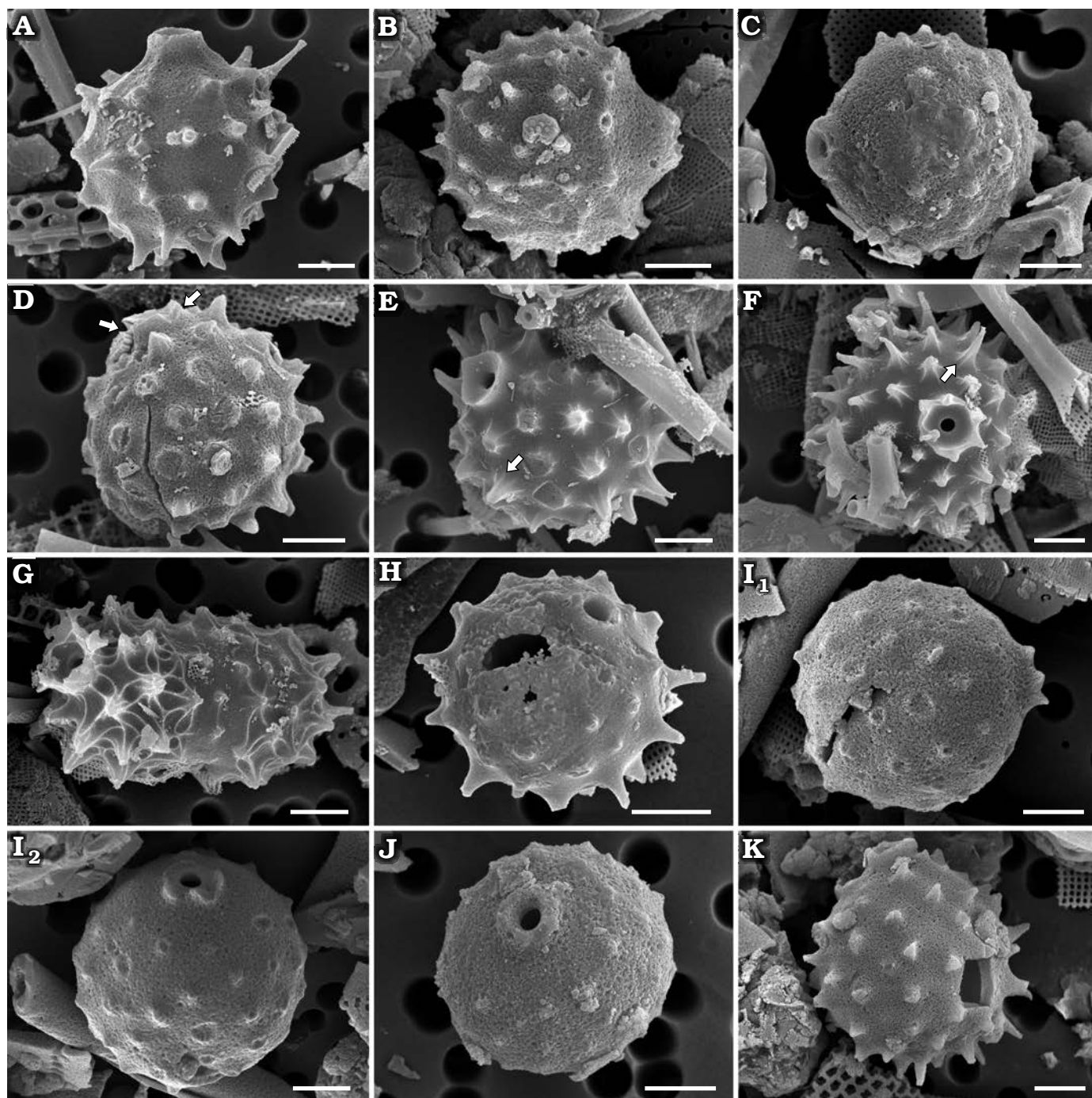


Fig. 6. Archaeomonad stomatocysts from Rupelian (lower Oligocene) of Poland. **A–C.** *Archaeomonas antioconica* Kaczmarek sp. nov. **A.** DMF stub 333-10 (KRAM A-32) holotype, Łubno 4, in lateral view with best preserved circumcollar spines. **B.** DMF stub 333-4, Borek Nowy 5A, in lateral view showing profile of anterior pole. **C.** DMF stub 342-14, Hermanowa 27, in antio-lateral view showing details of collar. **D.** *Archaeomonas japonica* Deflandre, 1933, DMF stub 333-10b, Łubno 4, in lateral view showing collar with uneven rim (arrows). **E–G.** *Archaeomonas karinae* Perch-Nielsen, 1978, Łubno 4. **E.** DMF stub 333-10c, in antio-lateral view, with typical spherical morphology with spines adorned with longitudinal ribs (arrow). **F.** DMF stub 333-18a, in anterior view, with typical spherical morphology with spines adorned with longitudinal ribs (arrow). **G.** DMF stub 333-18b, in antio-lateral view, with more ellipsoidal cell with more pronounced spine and collar morphology. **H–J.** *Archaeomonas manginii* Deflandre, 1932c, illustrating variation in preservation of spines and collars. **H.** DMF stub 342-13 (B 40 0046308), Łubno 4, in antio-lateral view, with eroded collar but well-preserved spines. **I.** DMF stub 349-16a, Futoma 4, stomatocyst with eroded spines but showing thickness and height of preserved collar rim, lateral (**I<sub>1</sub>**) and antio-lateral (**I<sub>2</sub>**) views. **J.** DMF stub 349-2f, Borek Nowy Kawalec, in antio-lateral view with eroded spines but showing thickness of collar rim. **K.** *Archaeomonas manginii* Deflandre, 1932c var. 1, DMF stub 349-17c, Futoma 4, in lateral view showing specimen with denser wall spines. Scale bars 2 µm.

rics of our specimens. In addition to spherical cysts, one ellipsoidal cyst was found with ribbed spines and similar

collar-pore apparatus (Fig. 6G). *Archaeomonas longispina* Rampi, 1948, is another species with stout interconnected



ribbed spines, but the spines appear relatively sparser and longer on the original figure for that species than on our specimens or *A. karinae*.

*Stratigraphic and geographic range*.—Eocene of the Vøring Plateau of the Norwegian Sea (Perch-Nielsen 1978), and Rupelian (lower Oligocene) of southeastern Poland (this study).

*Archaeomonas manginii* Deflandre, 1932c

Figs. 6H, I, J, K, 7A.

*Material*.—Numerous specimens encountered on each SEM stub from Borek Nowy 6, Kawalec (DMF stub 349-2f), Brzezówka 32, Futoma 4 (DMF stubs 349-16a, 349-17c, 349-17d), 5, 14, 17, 21, Łubno 4 (DMF stub 342-13 as B 40 0046308), Oligocene of southeastern Poland.

*Description*.—Stomatocysts spherical or subspherical, 3.3–9.0  $\mu\text{m}$  in diameter. Pores regular, 0.5–0.9  $\mu\text{m}$  in diameter (Fig. 6H, J). Collar cylindrical, low, with smooth to irregular margin, 1.0–2.5  $\mu\text{m}$  in diameter, up to 0.8  $\mu\text{m}$  high (Fig. 6I, K). Conulae or stout spines irregularly dispersed over cyst surface, less dense or absent near collar (Fig. 6I, J). Spines up to 1.0  $\mu\text{m}$  long and 0.9–3.1  $\mu\text{m}$  apart, or 3–11 in 10  $\mu\text{m}$ , most commonly 5–6 conulae/spines in 10  $\mu\text{m}$ .

Several slightly different specimens called *A. manginii* variant 1 (Figs. 6K, 7A), have a collar with several conulae. Their cell, pore, collar size, conulae and density overlap with typical variant described above (cell diameter 6.0–9.4  $\mu\text{m}$ , pores 0.6–0.7  $\mu\text{m}$ , collar up to 0.7  $\mu\text{m}$  high and 2.5  $\mu\text{m}$  in diameter). These cysts also covered with spines, 5–9 spines in 10  $\mu\text{m}$ . Spines fairly regularly dispersed with tendency to arrange into rows.

*Remarks*.—The size range of our specimens extends below that given in previous reports (6–10  $\mu\text{m}$ ) but meets other diagnostic criteria. Anterior pole spines and collar morphology shown on SEM images of the species in Deflandre and Deflandre-Rigaud (1969) and Stradner (1971) are also similar to our specimens. The presence of the narrow spineless area surrounding the collar is shown on the illustration of the holotype, but not on all specimens subsequently attributed to this species. Our specimens of *A. manginii* differ from *A. anterioconica* Kaczmarska sp. nov. by the rounded shoulders surrounding collar, spherical cyst outline, and low rim-like cylindrical collar. Freshwater Stomatocyst 31 Duff & Smol, 1989, illustrated in Duff et al. (1995) and Stomatocyst 157 Zeeb & Smol, 1993, show either similar spines, collar, or cell size, but in contrast to *A. manginii* and our specimens, the spines are equidistantly distributed on those cysts. *Archaeomonas manginii* is a relatively frequently reported species from sediments around the world.

*Stratigraphic and geographic range*.—Upper Cretaceous of the Moreno Formation, California (USA; Rampi 1940; Cornell 1972), Upper Cretaceous of the Subantarctic Southwest Pacific (Perch-Nielsen 1975), Eocene of the Kreyenhagen Formation, California (USA; Rampi 1969), Rupelian

(lower Oligocene) of southeastern Poland (this study), Miocene of the Calvert Formation, Maryland (USA; Tynan 1960; Deflandre 1932a), Miocene of Noto Peninsula (Japan; Bachmann 1964), Miocene of Limberg (Austria; Stradner 1971), and Tortonian (Miocene) of Hungary (Hajós 1968).

*Archaeomonas robusta* Rampi, 1969

Fig. 7B.

*Material*.—Numerous specimens encountered on each SEM stub from Futoma 4, 5, Łubno 3, 4 (DMF stub 342-13 as B 40 0046308), Oligocene of southeastern Poland.

*Description*.—Stomatocysts ovate, 14.3–18.7  $\mu\text{m}$  long and 11.6–14.6  $\mu\text{m}$  wide, widest at approximately one quarter of cyst length from posterior pole (Fig. 7B<sub>1</sub>). Pores surrounded by externally nearly cylindrical collar with spiny margins, up to 2.3  $\mu\text{m}$  high and 4.0–4.6  $\mu\text{m}$  in diameter. Internally to collar walls a flat planar annulus surrounds pore, 1.2–2.5  $\mu\text{m}$  in diameter (Fig. 7B<sub>2</sub>). Cyst wall surface slightly undulated by elevations covered with short stout conulae loosely organised into longitudinal rows, 1–3 rows in 10  $\mu\text{m}$ . Spines 1.2–1.6  $\mu\text{m}$  apart.

*Remarks*.—There are several ovate species with spiny walls recovered from marine sediments that are somewhat similar to our specimens. However, most have distinct, long cylindrical or slightly subconical collars (*A. cayeuxi* Deflandre, 1933, *A. verucosa* Rampi, 1969, *A. irregularis* Deflandre, 1932a) in addition to being significantly smaller and showing different patterns of spine distribution than seen on our specimens. In contrast, the original delineation of *A. robusta* states that the species ought to have "...wall thicker towards the pore where it forms a kind of neck. Surface rough, slightly undulating and dotted with small, low-lying pimples" (Rampi 1969: 7, translated from French). Although our specimens are just above the size attributed to *A. robusta*, the illustration of the holotype and other characters mentioned in the original species description fit them well. This species has been infrequently reported since its erection. Perch-Nielsen (1978) substantiates it with an image of a non-ovoid cyst with a long, narrow cylindrical collar, contrasting with the species delineation.

*Stratigraphic and geographic range*.—Eocene of the Kreyenhagen Formation, California (USA; Rampi 1969), Eocene of the Vøring Plateau of the Norwegian Sea (Perch-Nielsen 1978), and Rupelian (lower Oligocene) of southeastern Poland (this study).

*Archaeomonas* stomatocysts with equidistant wall protrusions

*Remarks*.—Equidistant distribution of wall surface protrusions (scabrae, papillae, conulae or spines) is relatively frequent among stomatocysts. Such stomatocysts are known from marine sediments since the Paleocene. For example, *Archaeomonas dubia*, *A. punctifera*, and *A. granulata* all share a quincunx, hexagonal or other grid-based pattern

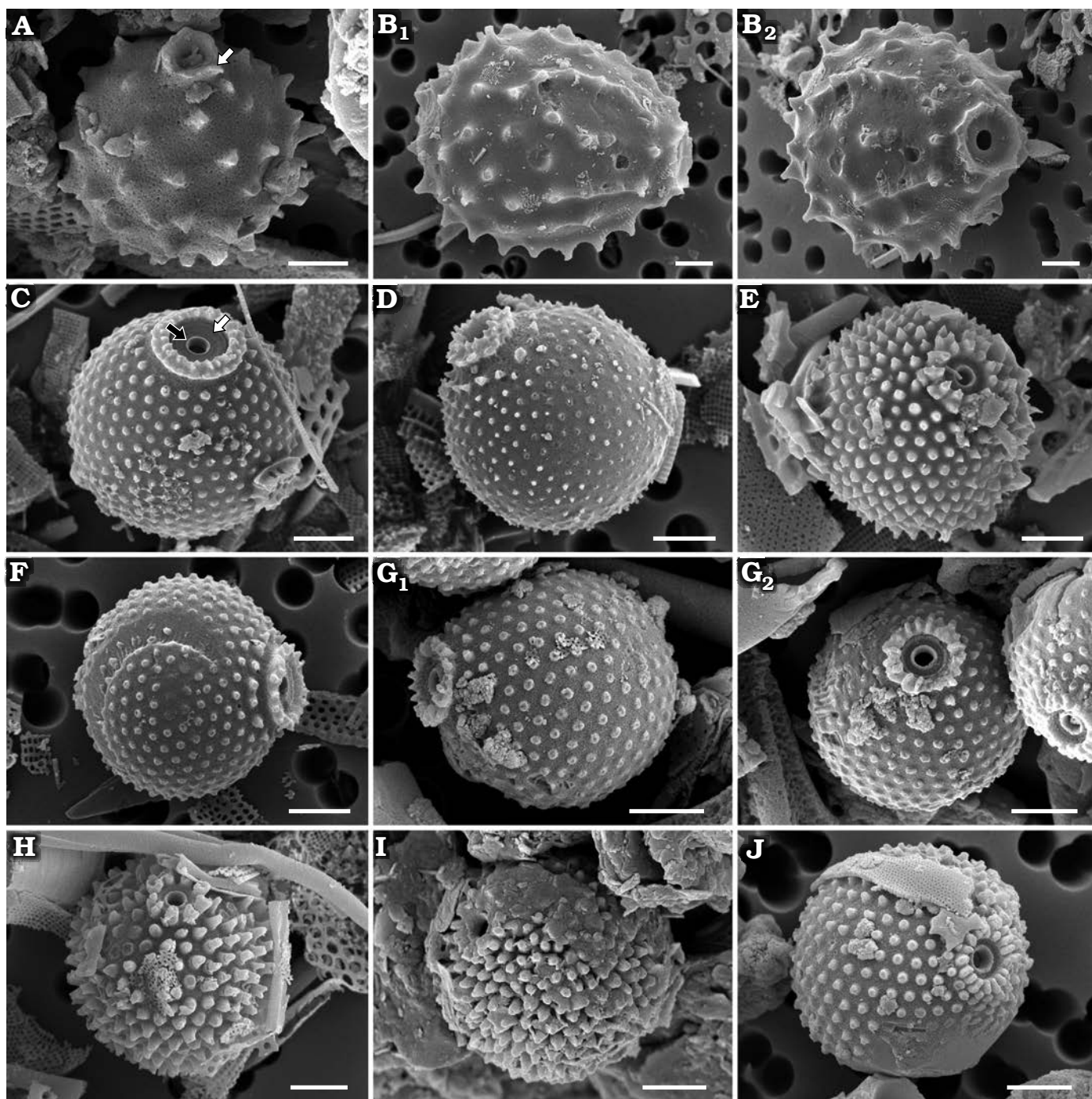


Fig. 7. Archaeomonad stomatocysts from Rupelian (lower Oligocene) of Poland (except I that is from Oligocene–Miocene, Canada). **A.** *Archaeomonas manginii* Deflandre, 1932c var. 1, DMF stub 349-17d, Futoma 4, in antero-lateral view showing less circular collar rim and several conulae (arrow). **B.** *Archaeomonas robusta* Rampi, 1969, DMF stub 342-13 (B 40 0046308), Łubno 4, in lateral view (**B<sub>1</sub>**), antero-lateral view showing pore structure (**B<sub>2</sub>**). **C–G.** *Archaeomonas jimstehrii* Ehrman & Kaczmarzka sp. nov. **C.** DMF stub 333-10 (KRAM A-33) holotype, Łubno 4, in antero-lateral view, with primary collar as low rounded marginal rim (black arrow) surrounded by planar interannulus (white arrow) and two rings of teeth in a secondary collar. **D.** DMF stub 333-10d, Łubno 4, in antero-lateral view, with two rings of teeth in a secondary collar. **E.** DMF stub 333-10e, Łubno 4, in antero-lateral view, with two rings of teeth in a secondary collar. **F.** DMF stub 342-10b, Łubno 3, in lateral view, with one ring of teeth. **G.** DMF stub 352-1g, Futoma 5, specimen with one ring of teeth, in lateral (**G<sub>1</sub>**) and anterior (**G<sub>2</sub>**) views. **H–J.** *Archaeomonas litheusphaerellamima* Samanta sp. nov. recovered from two spatially and temporally distant sites. **H.** DMF stub 333-10 (KRAM A-34), holotype, Łubno 4, in antero-lateral view. **I.** DMF stub 333-13, Oneida D-3, in antero-lateral view. **J.** DMF stub 352-2b, Futoma 5, in antero-lateral view. Scale bars 2  $\mu$ m.

of wall ornamentation (Deflandre and Deflandre-Rigaud 1969). Similarly, such stomatocysts are also known from extant inland and predominantly freshwater environments

(Duff et al. 1995; Wilkinson et al. 2001). They all differ from our three new species not only in collar structure (Stomatocyst 117 Zeeb et al., 1990; Stomatocyst 210



Duff & Smol, 1994; Stomatocyst 31 Duff & Smol, 1989; Stomatocysts 65, 67, 89 Van de Vijver & Beyens, 2000) but also in the size and shape of the surface structures (Stomatocyst 73 Duff & Smol, 1991) and their density (Stomatocyst 352 Zeeb & Smol, 2001 in Wilkinson et al. 2001).

*Archaeomonas jimstehrii* Ehrman & Kaczmarska  
sp. nov.

Fig. 7C–F, G.

PhycoBank ID: <http://phycobank.org/105039>.

Etymology: Dedicated to our son.

Holotype: DMF SEM stub 333-10, as preparation KRAM A-33, sample Łubno 4 (Fig. 7C, SEM image of stomatocyst in anterior-lateral view).

Type locality: Łubno, Poland.

Type horizon: Futoma Diatomite Member, Rupelian, lower Oligocene.

**Material.**—Stomatocysts with two rings of spines on secondary collar: Borek Nowy 5, Futoma 5 (DMF stub 352-1g), 17, Łubno 3, 4 (DMF stubs 333-10 as KRAM A-33, 333-10d, 333-10e). One ring of spines: Borek Nowy 5, Futoma 5 (DMF stub 352-1g), 14, 20, Łubno 3 (DMF stub 342-10b). Numerous specimens encountered on each SEM stub. All Oligocene of southeastern Poland.

**Diagnosis.**—Collar apparatus complex; primary collar low rounded marginal rim surrounded by wide planar interannulus. Secondary collar carries one or two rings of small spines and conulae.

**Description.**—Stomatocysts spherical, 6.2–8.4  $\mu\text{m}$  in diameter, including surface projections 0.5–0.8  $\mu\text{m}$  in diameter in well preserved specimens. Pores surrounded by complex collar apparatus. Two variants of the collar were found. Primary collar in form of low rounded marginal rim (Fig. 7C, E) is surrounded by a planar interannulus (Fig. 7C), which in turn is surrounded by secondary collar consisting of two rings (variant one, Fig. 7D) or a single ring (variant two, Fig. 7F, G<sub>1</sub>) of spines and conulae (Fig. 7E, F, G). In variant one, the primary collar height may reach 0.4  $\mu\text{m}$  with diameter 0.7–1.1  $\mu\text{m}$ . Secondary collar height may reach 0.8  $\mu\text{m}$  (including projections) and 2.0–3.3  $\mu\text{m}$  in diameter. Overall shape of secondary collar varies from cylindrical to obconical. Stomatocyst wall densely covered by nodules, up to 0.4  $\mu\text{m}$  high, organised into a pattern similar to nodes in a regular hexagonal lattice, 13–23 papillae in 10  $\mu\text{m}$ .

Metrics for variant two of these cysts overlap with those of the variant one described above: cysts 5.7–8.0  $\mu\text{m}$ , pores 0.5–0.7  $\mu\text{m}$  in diameter, primary collar 0.7–1.0  $\mu\text{m}$  and secondary 2.0–3.3  $\mu\text{m}$  in diameter, density of papillae 13–18 in 10  $\mu\text{m}$ . No specimens with intermediate collar morphologies were found.

**Remarks.**—Our specimens share some characters with three species of the genus *Archaeomonas*: *A. dubia* Deflandre, 1933, *A. punctifera* Deflandre, 1933, and *A. granulata* Rampi, 1969. All are similar in terms of cell and pore size and in their wall patterning. However, original descriptions

and available illustrations show quite different collar structures in all three species. In contrast to our specimens, *A. dubia* (Deflandre 1933; Deflandre and Deflandre-Rigaud 1969; Perch-Nielsen 1978) has a cylindrical, rounded rim-like collar. The collar in *A. punctifera* is very low, nearly indistinguishable from the structures covering the cyst surface, while the pore in *A. granulata* is surrounded only by a plain thick marginal rim (Rampi 1969).

**Stratigraphic and geographic range.**—Rupelian (lower Oligocene) of southeastern Poland (this study).

*Archaeomonas litheusphaerellamima* Samanta sp. nov.

Fig. 7H–J.

PhycoBank ID: <http://phycobank.org/105040>.

Etymology: From Latin *mimus* (actor, resembling others); due to superficial similarity to species from the genus *Litheusphaerella*.

Holotype: DMF SEM stub 333-10, as preparation KRAM A-34, sample Łubno 4 (Fig. 7H, SEM image of stomatocyst in anterior-lateral view).

Type locality: Futoma, Poland.

Type horizon: Futoma Diatomite Member, Rupelian, lower Oligocene.

**Material.**—Numerous specimens found on each SEM stub from Borek Nowy 5, Futoma 5 (DMF stub 352-2b), Łubno 4 (DMF stub 333-10 as KRAM A-34), Oligocene of southeastern Poland. Additionally several specimens on Canadian preparation (DMF stub 333-13) from Shell Oneida O-25 well (CGS D-3), Scotian Shelf, Canadian waters, lower Miocene.

**Diagnosis.**—Secondary collar adorned with bacculate and bifurcate spines, remaining cyst surface covered with solid, stout pointed spines in regular, hexagonal grid. Planar interannulus present.

**Description.**—Stomatocysts spherical, 7.3–9.1  $\mu\text{m}$  in diameter, densely covered by regularly distributed solid, stout pointed spines (Fig. 7H, I). Undamaged spines 0.6–0.8  $\mu\text{m}$  long, positioned nearly equidistantly, 9–20 in 10  $\mu\text{m}$  in hexagonal grid. Regular pores 0.5–0.6  $\mu\text{m}$  in diameter surrounded by complex collar system. Primary collar cylindrical, surrounded by flat planar interannulus, followed by ring of 9–18 columnar spines (Fig. 7J). Free ends of collar spines flat or bifurcated.

**Remarks.**—This distinct stomatocyst is superficially similar to *Litheusphaerella spectabilis* Deflandre, 1932c, in carrying regularly and equidistantly distributed spines. However, the spines in our species are stout, short, and pointed. Moreover, spines in our species lack a hollow center and the T-shaped apices which are characteristic of *L. spectabilis*. This can be seen on images shown by Perch-Nielsen (1978) and our own specimens presented below in the last section of the results. The collar-pore apparatus in our specimens is also different from that shown for *L. spectabilis* on SEM images of cells recovered from the type locality (Deflandre and Deflandre-Rigaud 1969). Diagnostic characters described for the new species are stable. In addition to the Polish Rupelian diatomites, we found this species in the interval between 1575–1610 feet (480–491 m) below the seafloor in the Shell



Oneida 0-25 well (GSC locality D-3; at 43° 14' 57.36" N, 61° 33' 36.49" W) taken near the Scotian Shelf edge, Atlantic coast of Canada (IK unpublished data; Fig. 7I). These strata correspond to the Lower Miocene series (Barss et al. 1979).

*Stratigraphic and geographic range*.—Rupelian (lower Oligocene) of southeastern Poland (this study), and Lower Miocene, Scotian Shelf (Atlantic coast of Canada; IK unpublished data).

*Archaeomonas sextapapillatus* Kaczmarek sp. nov.

Fig. 8A, B, C, D, E–G.

*Phycobank ID*: <http://phycobank.org/105041>.

*Etymology*: Reflects the hexagonal pattern of the cyst wall ornamentation.

*Holotype*: DMF SEM stub 352-1, as preparation KRAM A-31, sample Futoma 5, fine fraction (Fig. 8G, SEM image of stomatocyst in anterior-lateral view).

*Type locality*: Futoma, Poland.

*Type horizon*: Futoma Diatomite Member, Rupelian, lower Oligocene.

*Material*.—Several specimens encountered on each SEM stub from Borek Nowy 5, Futoma 4 (DMF stubs 349-17e, 349-17f, 349-17g), 5 (DMF stubs 252-1h, 352-1i, 352-2c, 352-1 as KRAM A-31), 14, Łubno 2, 4, Oligocene of southeastern Poland.

*Diagnosis*.—Complex, conical, multilayered secondary collar with the outermost layer overlaying the secondary collar original external surface, carrying one or two rings of papilla. Primary collar in the form of narrow rim. Planar interannulus present.

*Description*.—Stomatocysts spherical, 6.0–8.6 µm in diameter, including papillae. Regular pore diameter 0.4–0.8 µm in well preserved specimens. Pores surrounded by complex collar apparatus. Primary collar in form of narrow marginal rim (0.6–0.9 µm in diameter, Fig. 8E) and surrounded by a planar interannulus (Fig. 8E). These in turn surrounded by a gently conical secondary collar, 1.3 µm in apical and 3.4 µm in basal diameter (Fig. 8B). Secondary collar 0.4–1.1 µm high. In some cysts, additional layer of silica overlays secondary collar, covering it with a folded-out from the top layer that may be smooth (Fig. 8C<sub>1</sub>, D<sub>1</sub>, E) or carry small papillae on its surface (Fig. 8A, B, F, and G). Stomatocyst wall densely covered by stout papillae in a regular hexagonal lattice pattern, up to 0.8 µm high, 13–22 papillae in 10 µm. Figures 8B, C, D, E–G show progression of buildup (or erosion) of pore-collar system with folded-over layer covering external surface of secondary collar base and cyst surface.

*Remarks*.—Somewhat similar to our specimens are those of *A. multipunctata* Rampi, 1969, shown by Perch-Nielsen (1978). However, the illustration in Rampi (1969) presents cells with less regularly distributed papillae and a simple rim-collar. *Archeomonas sextapapillatus* Kaczmarek sp. nov. size and wall ornamentation are similar to *A. jimstehrii* Ehrman & Kaczmarek sp. nov. but the two differ in the structure of the secondary collar, clearly demonstrated in

Fig. 8A; *A. jimstehrii* Ehrman & Kaczmarek sp. nov. on the left and *A. sextapapillatus* Kaczmarek sp. nov. on the right.

*Stratigraphic and geographic range*.—Rupelian (lower Oligocene) of southeastern Poland (this study).

*Archaeomonas* stomatocysts with smooth walls

*Remarks*.—We note that some freshwater cysts of similar, smooth-wall morphology are thought to represent early developmental stages of several species whose mature stomatocysts walls will eventually become different (Duff et al. 1995; Wilkinson et al. 2001; Holen 2014). For example, the smooth-walled Stomatocyst 234 Duff et al., 1995, may represent several members of the genus *Paraphysomonas* De Saedeleer, 1929 (Duff et al. 1995; Bai et al. 2023), or a species of *Dermatochrysis* (Holen 2014). There may be similar examples among species found in marine environments. Furthermore, some haptophyte species recovered from decades old marine sediments also produced cysts similar to smooth-walled chrysophytes (Ellegaard et al. 2016). Due to these uncertainties, we refrain from describing any new species of stomatocysts with indistinct collars and smooth walls.

*Archaeomonas* aff. *inconspicua* Deflandre, 1933

Fig. 8H.

*Material*.—Several specimens encountered on each SEM stub from Borek Nowy 5, 12, Futoma 5 (DMF stub 352-1j), 17, Oligocene of southeastern Poland.

*Description*.—Stomatocysts spherical or slightly oblate (when infrequently observed in lateral view), 3.0–11.0 µm in diameter. Cyst external wall surface smooth, no collar. Pores conical, 0.7–2.0 µm in outer and 0.4–1.1 µm in inner diameter (Fig. 8H). Smaller cysts have proportionally smaller pores.

*Remarks*.—The current delineation of *A. inconspicua* is sufficiently general to encompass the smaller of our specimens. Cysts presented by Deflandre (1933) and Tynan (1960) were only 3–5 µm in diameter, although Hajós (1968) reported cells up to 7 µm in diameter. However, neither Deflandre nor Tynan provided details of pore size and structure, so we attribute our specimens to this species with reservations. There are also stomatocysts reported from freshwater environments that are quite similar to our specimens. Examples are Stomatocyst 29 Duff & Smol, 1989, emended in Zeeb and Small (1993), Stomatocyst 120 Zeeb & Smol, 1993, and Stomatocyst 42 Duff & Smol, 1989, and immature cysts which are well delineated and illustrated in Duff et al. (1995) and Holen (2014). Basic differentiation of the three cysts rests on their diameters (3–5.9 µm, 6.0–8.9 µm, and 9.0+ µm, respectively) and all fall within the size range of our specimens. See also our closing remarks at the end of the section devoted to smooth-walled stomatocysts.

*Archaeomonas kreyenhagenensis* Rampi, 1969

Fig. 8I, J.

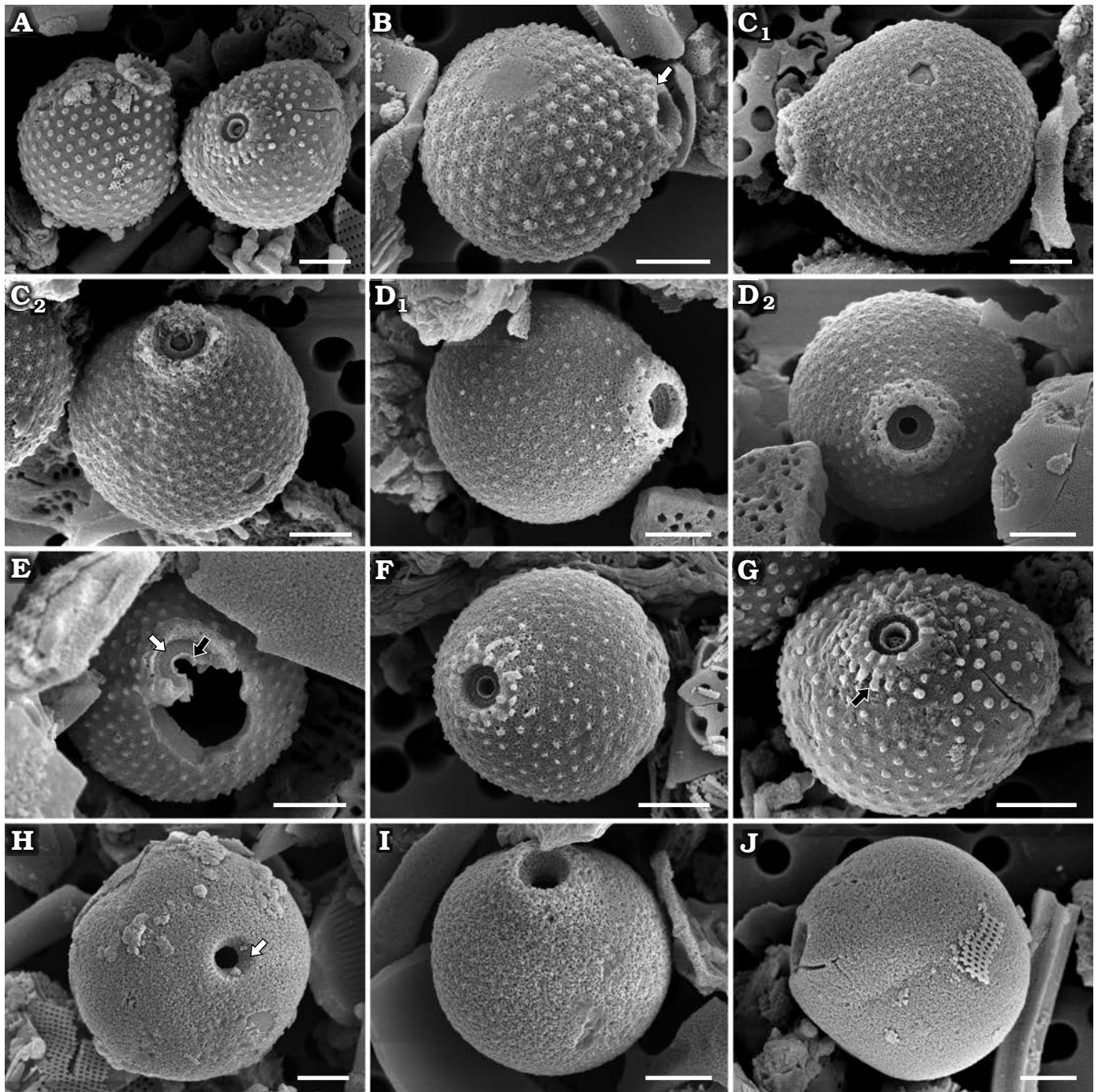


Fig. 8. Archaeomonad stomatocysts from Rupelian (lower Oligocene) of Poland. A–G. *Archaeomonas sextapapillatus* Kaczmarzka sp. nov. A. Comparison of *A. sextapapillatus* Kaczmarzka sp. nov. (right cell in antero-lateral view) with *A. jimstehrii* Ehrman & Kaczmarzka sp. nov. (left cell in lateral view) illustrating difference in collar structure, DMF stub 352-1h, Futoma 5. B–G. Specimens demonstrating increasingly complex collar system, due to development and/or preservation (see text). B. DMF stub 352-1i, Futoma 5, in lateral view showing gently conical secondary collar (arrow). C. DMF stub 349-17e, Futoma 4, in lateral (C<sub>1</sub>) and antero-lateral (C<sub>2</sub>) views. D. DMF stub 349-17f, Futoma 4, in antero-lateral (D<sub>1</sub>) and anterior (D<sub>2</sub>) views. E. DMF stub 352-2c, Futoma 5, in anterior view showing narrow marginal rim (black arrow) surrounded by planar interannulus (white arrow). F. DMF stub 349-17g, Futoma 4, in antero-lateral view. G. DMF stub 352-1 (KRAM A-31), holotype, Futoma 5, in antero-lateral view, showing small papillae on secondary collar present on some statocysts (arrow). H. *Archaeomonas* aff. *inconspicua* Deflandre, 1933, DMF stub 352-1j, Futoma 5, in anterior view showing conical pore (arrow). I, J. *Archaeomonas kreynhagenensis* Rampi, 1969, Futoma 5. I. DMF stub 352-1k, in antero-lateral view showing pore and collar. J. DMF stub 352-1l, in lateral view. Scale bars 2  $\mu$ m.

**Material.**—Numerous specimens encountered on each SEM stub from Borek Nowy 5, Futoma 5 (DMF stubs 352-1k, 352-1l), Łubno 4, Oligocene of southeastern Poland.

**Description.**—Stomatocysts slightly ovate in lateral view (Fig. 8J) and spherical in anterior or posterior orientation, 6.0–8.6  $\mu$ m in diameter. Anterior ends slightly and grad-



ually attenuated, but no distinct collar is apparent. Visible part of pores obconical (Fig. 8I), 0.7–0.8  $\mu\text{m}$  in basal diameter, widening towards cyst external surface to 1.5–2.2  $\mu\text{m}$  in diameter. Cysts walls smooth.

*Remarks.*—Overall outline of the cysts, specifically wide and gently attenuating anterior poles, meets the species delineation. The bi-conical structure of the pores visible in LM cannot be readily observed using SEM. However, the obconical area above the narrowest part of the pore, the perforation of the cyst wall, was repeatedly observed. Californian stomatocysts (Rampi 1969) were also slightly larger than our cysts: 9.5  $\mu\text{m}$  vs. 6–8.5  $\mu\text{m}$  in diameter, respectively.

*Stratigraphic and geographic range.*—Upper Cretaceous of the Subantarctic Southwest Pacific (Perch-Nielsen 1975), Eocene of the Kreyenhagen Formation, California (USA; Rampi 1969), Upper Eocene of the Vøring Plateau of the Norwegian Sea (Perch-Nielsen 1978), and Rupelian (lower Oligocene) of southeastern Poland (this study).

#### *Archaeomonas* cf. *mamillosa* Tynan, 1960

Fig. 9A.

*Material.*—Several specimens encountered on each SEM stub from Futoma 5 (DMF stub 352-1m), Łubno 2, Oligocene of southeastern Poland.

*Description.*—Stomatocysts spherical, 4.5–5.6  $\mu\text{m}$  in diameter with smooth surface (Fig. 9A). Regular pores 0.4–0.6  $\mu\text{m}$  in diameter, surrounded by low collar in form of rounded marginal rim, 1.0–1.3  $\mu\text{m}$  in diameter.

*Remarks.*—In most of the characters except cell size, our specimens are similar to *A. mamillosa*. However, those cysts are nearly twice as large as our specimens. The extant freshwater Stomatocyst 51 (Duff & Smol in Duff et al., 1995), are similar in size but have larger pores.

#### *Archaeomonas simplicia* Rampi, 1969

Fig. 9B.

*Material.*—Several specimens found on each SEM stub from Borek Nowy Kawalec (DMF stub 349-2g), Futoma 5, Oligocene of southeastern Poland.

*Description.*—Stomatocysts slightly oblate or spherical, depending on cyst orientation, 3.6–7.1  $\mu\text{m}$  wide and 4.1–7.5  $\mu\text{m}$  long (Fig. 9B). Cyst wall surface smooth. Distinct collar clearly offset from wall surface. Collar conical, up to 0.7  $\mu\text{m}$  high (may depend on preservation) and 1.3–2.7  $\mu\text{m}$  in basal diameter, depending on cyst size.

*Remarks.*—The size range of our specimens is smaller than the 7–8  $\mu\text{m}$  diameter given by earlier work (Rampi 1969). As well, the collar of our stomatocysts appears proportionally wider with respect to the cyst diameter than those illustrated by Rampi (1969) and Deflandre and Deflandre-Rigaud (1969). Similar species with smooth wall surfaces are *A. colligera* Hajós, 1968, and to a lesser extent *A. pseudocompressa* Hajós, 1968. *Archaeomonas colligera* is similar to our specimens in collar morphology but those cysts are ellipsoidal and

larger while *A. pseudocompressa* is also larger with cylindrical, not conical collars.

*Stratigraphic and geographic range.*—Upper Cretaceous of the Moreno Formation, California (USA; Rampi 1940), Upper Cretaceous of the Subantarctic Southwest Pacific (Perch-Nielsen 1975), Eocene of the Kreyenhagen Formation, California (USA; Rampi 1969), Upper Eocene of the Vøring Plateau of the Norwegian Sea (Perch-Nielsen 1978), and Rupelian (lower Oligocene) of southeastern Poland (this study).

#### *Archaeomonas sphaerica* Deflandre, 1932a

Fig. 9C.

*Material.*—Numerous specimens found on each SEM stub from Futoma 4 (DMF stub 349-17h), 5, 14, 16, Hermanowa 27, Łubno 3, Oligocene of southeastern Poland.

*Description.*—Stomatocysts spherical with smooth external walls (Fig. 9C). Two size-classes of specimens: 5.6–6.5  $\mu\text{m}$  and 10–11.5  $\mu\text{m}$  in diameter. Collar absent. Regular pores 0.8–1.3  $\mu\text{m}$  and 1.1–1.7  $\mu\text{m}$  in diameter in smaller and larger cysts, respectively. Pores in both size-classes of cyst descend sharply, directly, and nearly unchanged in diameter through cyst wall into its interior.

*Remarks.*—Specimens attributed to this species by Deflandre and Deflandre-Rigaud (1969) encompass a somewhat greater range of sizes (11–12  $\mu\text{m}$  in diameter) than in the original description. The images obtained using SEM clearly illustrate the lack of a collar and the regular form of the pores. Although some of our specimens exceed the cell size range of the original delineation for *A. sphaerica*, their pore morphology is consistently similar, thus we attribute all our specimens to this species. In contrast, among the smooth-surface spherical stomatocysts with no collar and regular pores found in the freshwater environment, Duff et al. (1995) differentiate three separate stomatocysts types: Stomatocysts 1, 9, 15 Duff et al., 1995. Diameters of these cysts range from  $\leq 5.9 \mu\text{m}$ , 6.0–8.9  $\mu\text{m}$ , and  $\geq 9.0 \mu\text{m}$  in diameter, respectively. Strictly adhering to those size criteria, our specimens span all three stomatocyst types. See also our closing remarks at the end of smooth-walled stomatocysts section.

*Stratigraphic and geographic range.*—Paleocene/Eocene boundary of Fuur Island, North Jutland (Denmark; Deflandre 1932a), Rupelian (lower Oligocene) of southeastern Poland (this study), Tortonian (Miocene) of Hungary (Hajós 1968), and Miocene of the Vøring Plateau of the Norwegian Sea (Perch-Nielsen 1978).

#### *Archaeomonas* aff. *sphaerica* Deflandre, 1932a

Fig. 9D.

*Material.*—Numerous specimens found on each SEM stub from Futoma 4, 5, 17, Łubno 4 (DMF stub 333-18c), Oligocene of southeastern Poland.

*Description.*—Stomatocysts with outline varying from slightly to more distinctly oblate, although difference be-

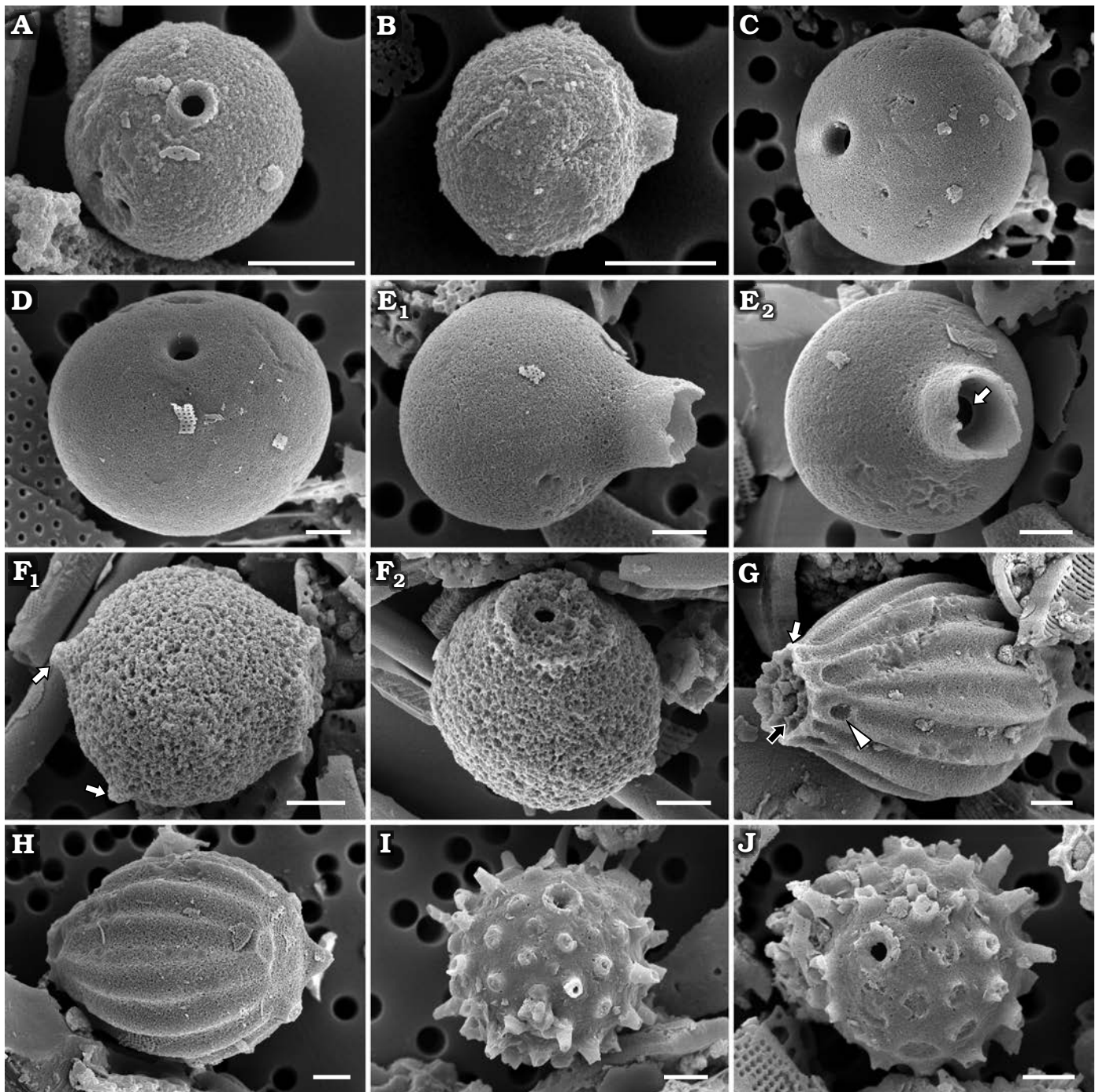


Fig. 9. Archaeomonad stomatocysts from Rupelian (lower Oligocene) of Poland. **A.** *Archaeomonas* cf. *mamillosa* Tynan, 1960, DMF stub 352-1m, Futoma 5, in anterior view. **B.** *Archaeomonas simplicia* Rampi, 1969 DMF stub 349-2g, Borek Nowy Kawalec, in lateral view. **C.** *Archaeomonas sphaerica* Deflandre, 1932a, DMF stub 349-17h, Futoma 4, in antero-lateral view. **D.** *Archaeomonas* aff. *sphaerica* Deflandre, 1932a, DMF stub 333-18c, Łubno 4, in antero-lateral view. **E.** *Archaeomonas tubulata* Deflandre, 1938, DMF stub 352-1n, Futoma 5, in lateral view (**E<sub>1</sub>**), antero-lateral view (**E<sub>2</sub>**), looking into the tubular collar, showing pore surrounded by flat planar annulus (arrow). **F.** *Archaeosphaeridium australensis* Perch-Nielsen, 1975, DMF stub 352-1o, Futoma 5, in lateral view showing prominent posterior spines (**F<sub>1</sub>**, arrows), antero-lateral view showing characteristically wide collar (**F<sub>2</sub>**). **G, H.** *Litharchaeocystis centparatethianus* Ehrman sp. nov. **G.** DMF stub 349-17i, Futoma 4, in antero-lateral view, showing structure of collar system with inner layer (black arrow), outer layer (white arrow), and arches in basal part of collar with windows in between (arrowhead). **H.** DMF stub 333-10 (KRAM A-35), holotype, Łubno 4, in postero-lateral view showing details of flattened posterior pole. **I, J.** *Litheusphaerella spectabilis* Deflandre, 1932c, Borek Nowy 12B. **I.** DMF stub 342-15c, in antero-lateral view showing characteristic collar. **J.** DMF stub 342-15d, in anterior view showing collar and hollow spines. Scale bars 2  $\mu$ m.

tween cyst width and length varies only between 0.4–1.6  $\mu$ m; from 5.2–10.9  $\mu$ m in short to 6.2–12.6  $\mu$ m in long axis (Fig. 9D). Regular pores 0.6–0.9  $\mu$ m in inner and 0.9–1.5  $\mu$ m in outer diameter in best preserved and oriented specimens.



*Remarks.*—We are not aware of a marine archaeomonad species with the characteristics of our specimens, particularly given the variation in the cyst outline, with individuals grading from slightly to clearly oblate. The common character of our specimens is a regular pore, similar to those in our specimens of *A. sphaerica*. Among the freshwater stomatocyst types with similar overall morphology of the cyst-body, all have more elaborate pore structures and collars. See also our closing remarks at the end of smooth-walled stomatocysts section.

### *Archaeomonas tubulata* Deflandre, 1938

Fig. 9E.

*Material.*—Only one specimen from Futoma 5 (DMF stub 352-1n), Oligocene of southeastern Poland.

*Description.*—One slightly oval stomatocyst found, 8.3  $\mu\text{m}$  wide and 9.4  $\mu\text{m}$  long. Cyst wall surface smooth. Distinct collar clearly offset from wall surface. Collar tubular, up to 2.0  $\mu\text{m}$  in height, may be longer as it appears broken (Fig. 9E<sub>1</sub>). Collar relatively wide, cylindrical, 3.1–3.4  $\mu\text{m}$  in basal diameter. Pore 1.3  $\mu\text{m}$  in diameter surrounded by narrow flat planar annulus (Fig. 9E<sub>2</sub>).

*Remarks.*—Our specimen is larger than in the original description (5.9  $\mu\text{m}$  in diameter calculated from an image shown by Deflandre 1938), but *A. tubulata* is the only species known to us that possesses such a long, straight tubular collar. Perch-Nielsen (1978) illustrates a specimen with a relatively long collar but attributes it to *A. simplicia*.

*Stratigraphic and geographic range.*—Rupelian (lower Oligocene) of southeastern Poland (this study), and Miocene of the Marmorito diatomites (Italy; Deflandre 1938; Deflandre and Deflandre-Rigaud 1969).

## Other genera

### Genus *Archaeosphaeridium* Deflandre, 1932c

*Type species:* *Archaeosphaeridium dangeardianum* Deflandre, 1932c. Miocene, Poplein, Calver County, Maryland (USA).

### *Archaeosphaeridium australensis* Perch-Nielsen, 1975

Fig. 9F.

*Material.*—Several specimens encountered on SEM stub from Futoma 5 (DMF stub 352-1o), Oligocene of southeastern Poland.

*Description.*—Stomatocysts 8.2–9.0  $\mu\text{m}$  in diameter, spherical to slightly oblate, depending on cyst orientation. Cyst wall smooth except for two (notable) posterior spines, represented here only by their bases (Fig. 9F<sub>1</sub>). Regular pores, 0.8  $\mu\text{m}$  in diameter (Fig. 9F<sub>2</sub>). Collar large, smooth, with wide, flat marginal rim, 4.4  $\mu\text{m}$  in diameter at base.

*Remarks.*—Perch-Nielsen (1975) erected a new species made distinct by the small number of downward pointing posterior spines and short, large collar. These characters differentiated the species from those previously known in this genus and

two others described by her at the same time. Our specimens meet all morphological criteria for *A. australensis* except cyst size, which is smaller than her mostly commonly encountered cysts of 15–20  $\mu\text{m}$  in diameter. Similar to our specimens, Gombos (1977) also found this species in the same time interval.

*Stratigraphic and geographic range.*—Upper Eocene to lower Oligocene of the Subantarctic Southwest Pacific (Perch-Nielsen 1975), Upper Eocene to lower Oligocene of the Malvinas Outer Basin, South Atlantic Ocean (Gombos 1977), and Rupelian (lower Oligocene) of southeastern Poland (this study).

### Genus *Litharchaeocystis* Deflandre, 1932b

*Type species:* *Litharchaeocystis costata* Deflandre, 1932b. Marine fossil deposits at Kuznetsk (Russia). No specific age given in Deflandre (1932b), but age was indicated in Deflandre and Deflandre-Rigaud (1969) as Paleocene–Eocene.

### *Litharchaeocystis centparatethianus* Ehrman sp. nov.

Fig. 9G, H.

*Phycobank ID:* <http://phycobank.org/105042>.

*Etymology:* Refers to the name of the ancient basin Central Paratethys in which the species is found.

*Holotype:* DMF SEM stub 333-10, as preparation KRAM A-25d, sample Łubno 4 (Fig. 9H, SEM image of stomatocyst in anterior-lateral view).

*Type locality:* Futoma, Poland.

*Type horizon:* Futoma Diatomite Member, Rupelian, lower Oligocene.

*Material.*—A few specimens encountered on each SEM stub from Futoma 4 (DMF stub 249-17i), Łubno 4 (DMF stub 333-10 as KRAM A-35), Oligocene of southeastern Poland.

*Diagnosis.*—Ellipsoidal cyst with relatively fine ridges and flaring collar. Collars two-layered. Inner and outer layers connected by septa. Basal part of collar outer wall arches to connect with some surface ridges leaving windows in between.

*Description.*—Stomatocysts ellipsoidal, anterior end tapering to two-layered collar. Cells 15.1–16.5  $\mu\text{m}$  long and 11.0–11.4  $\mu\text{m}$  wide at their widest portion. Cyst surface adorned by sharp longitudinal ridges running cell length, approximately 4 ridges in 10  $\mu\text{m}$ . Nine ridges present over visible side of cysts. In appropriate orientation approximately 4 ridges associate with each short, wide-based posterior spine (Fig. 9G). Cyst posterior end flattened and surrounded by a ring of at least 4 stout spines, 1.5–2.1  $\mu\text{m}$  long (Fig. 9H). Collar system complex, two-layered. Inner (primary?) and outer layer (Fig. 9G) connected to each other by perpendicular septa. Collar-system inner layer is conical while outer obconical. Basal part of collar outer layer arches to connect with some surface ridges leaving windows in between (Fig. 9G), thus not grounded on cyst surface. Both layers have serrated apical margins.

*Remarks.*—Our specimens meet the generic delineation (Deflandre 1932b), but not any of the currently known

species. In addition to the different pattern of ridges and structure of collars, it differs by being more ellipsoidal in shape compared to triangular, bottom-heavy outlines of *Litharchaeocystis glabra* Rampi, 1948, *L. oamaruensis* Deflandre, 1938, *L. talwanii* Perch-Nielsen, 1978, or *L. udintsevii* Perch-Nielsen, 1978. Our species is not as ellipsoidal as *L. costata* Deflandre, 1932b, from which it also differs by being much smaller (31–34  $\mu\text{m}$  vs. 15.5–16.5  $\mu\text{m}$  long; 18–20  $\mu\text{m}$  vs. 11.0–11.4  $\mu\text{m}$  wide) and having a greater number of ridges on the visible side of the cysts (9 vs. 6, respectively). All the species mentioned above are reported from sediments from New Zealand, Russia, and the Vøring Plateau of the Norwegian Sea (Deflandre and Deflandre-Rigaud 1969; Perch-Nielsen 1978).

*Stratigraphic and geographic range.*—Rupelian (lower Oligocene) of southeastern Poland (this study).

### Genus *Litheusphaerella* Deflandre, 1932c

*Type species:* *Litheusphaerella spectabilis* Deflandre, 1932c. Paleocene/Eocene boundary, Fuur Island, North Jutland (Denmark).

#### *Litheusphaerella spectabilis* Deflandre, 1932c (sensu lato)

Fig. 9I, J.

*Material.*—Numerous specimens encountered on each SEM stub from Borek Nowy 5, 12B (DMF stubs 342-15c, 342-15d), Futoma 5, 17, Łubno 2. Oligocene of southeastern Poland.

*Description.*—Stomatocysts spherical, 7.8–11.2  $\mu\text{m}$  in diameter when measured with spines. Pores approximately 1  $\mu\text{m}$  in diameter, surrounded by low, narrow ring of obconical collar, 1.5–2.0  $\mu\text{m}$  in total diameter. Spines long, robust and widest at base. Longest spines found have broken tips but reach 1.7  $\mu\text{m}$  in length. Spines hollow throughout length but occluded at base (Fig. 9I). Spines regularly dispersed, generally equidistant from each other, 1.8–2.0  $\mu\text{m}$  apart. Narrow spineless ring around collar (Fig. 9J).

*Remarks.*—Our specimens are most like SEM images published by Deflandre and Deflandre-Rigaud (1969) from the Lower Eocene of Jutland (Denmark) with both hollowed spines and pore-collar apparatus. Not all such details are obvious on micrographs or drawings of the species published by all authors (Perch-Nielsen 1975, 1978; Stradner 1971) supporting the notion that *L. spectabilis* as currently delineated may encompass more than one species (Deflandre 1932c). There are also reported extant specimens attributed to *L. spectabilis* (Mitchell and Silver 1982) while Riaux-Gobin and Stumm (2006, as *L. cf. spectabilis*) considered their specimens similar to this species but not without reservations. Somewhat similar specimens are presented by Kato (2019), as Stomatocyst 65 Van de Vijver & Boyens, 2000, but the density of the spines is greater than the density of spines on our specimens.

*Stratigraphic and geographic range.*—Upper Cretaceous

of the Subantarctic Southwest Pacific (Perch-Nielsen 1975), Paleocene/Eocene boundary of Fuur Island, North Jutland (Denmark; Deflandre 1932a), Eocene of the Issinsky-Volga Region (Russia; Deflandre and Deflandre-Rigaud 1969), Eocene of the Vøring Plateau of the Norwegian Sea (Perch-Nielsen 1978), Rupelian (lower Oligocene) of southeastern Poland (this study), Miocene of Limberg (Austria; Stradner 1971). Recent reports from the Equatorial Pacific, North Pacific, and South Atlantic (Mitchell and Silver 1982), the Weddell Sea (Mitchell and Silver 1986), and Kita-no-seto Strait, Antarctica (Takahashi et al. 1986).

## Discussion

Due to structural similarities, archaeomonads have long been regarded as representing resting stages of flagellated freshwater chrysophytes (Deflandre 1932c; Mitchell and Silver 1986; Lipps and McCartney 1993). However, the recent discovery of morphologically similar resting cysts among marine haptophytes (Ellegaard et al. 2016) raises the question whether all marine archaeomonads represent chrysophytes. Species identification in both these algae is based on live vegetative cells that rarely preserve in the fossil record. In addition to non-mineralising species, both groups contain species whose vegetative cells are covered by usually more than one type of delicate siliceous scale (Graham et al. 2008; Yoshida et al. 2006; Abe et al. 2016) which in older sediments also fossilise exceptionally rarely (Siver 2020). In contrast, only one strongly silicified cyst is produced by one vegetative cell (Kristiansen and Andersen 1986; Holen 2014; Ellegaard et al. 2016). Moreover, the morphology of mature stomatocysts is thought to be species-specific (Kristiansen and Andersen 1986; Duff et al. 1995). Therefore, it is unlikely that a significant number of fossilised stomatocysts can be reconciled with their vegetative cell remains, so these soft life history characters can not contribute to routine species identification in fossilised material.

For decades archaeomonads were thought to have gone extinct during the Pliocene and thus absent in modern seas. Mitchell and Silver (1982, 1986) were first to recover living pelagic cysts apparently conforming to descriptions of four archaeomonad morphospecies. They were found in Antarctic seawater, sea-ice and seafloor sediments. Since then, other researchers have found similar stomatocysts in marine and brackish waters and underlying sediments (Buck and Garrison 1983; Andrén et al. 1999; Rull and Vegas-Vilarrúbia 2000; Hällfors 2004). Among those, the most reported cysts are similar to Miocene–Pliocene *Archaeomonas areolata* and Cretaceous–Miocene *Litheusphaerella spectabilis*. Unfortunately, the living specimens of these and other presumptive “living archaeomonad fossils” are yet to be appraised in comparison to the taxonomic-type material. Nonetheless, living stomatocysts of such affinity also allow the exciting opportunity to molecularly examine their phylogenetic relationships.



Research interest in archaeomonads has been sporadic. Most work was conducted between 1932 and the late 1970s as compared to the past five decades. Only 119 species were known by 1971 (Tynan 1971) and very few have been added since. Upper Cretaceous, Eocene, and Miocene floras are considered the most species rich (Table 1). For example, the Eocene sediments from the Vøring Plateau of the Norwegian Sea contain 25 species (Perch-Nielsen 1978), while 27 species were found in Tortonian sediments of the Upper Miocene in Hungary (Hajós 1968). Recently, even more diverse flora has been reported in the Upper Miocene–Pliocene sediments from the Atlantic section of the Southern Ocean (Kato 2019). Oligocene stomatocysts were unknown before 1971 (Tynan 1971) and there are still only a few reports from lower Oligocene sediments documenting them: three species from the Vøring Plateau of the Norwegian Sea and six from the Subantarctic Southwestern Pacific and Atlantic (Perch-Nielsen 1975, 1978; Gombos 1976). As far as we can determine, no archaeomonad has previously been reported from the Oligocene Central Paratethys. In this initial report, we document unanticipated species diversity of these cysts in Rupelian (lower Oligocene) diatomites at five sites in southeastern Poland, including 27 previously described taxa and 8 species new to science. Furthermore, at least a dozen additional distinct stomatocyst types were found in orientations and/or quantities insufficient to confidently describe them and so are not included in this presentation.

The biostratigraphic and palaeoceanographic significance of marine stomatocysts is difficult to assess due to the small number of studies and known species. It is unlikely that there are more than three hundred such species described to date. Nonetheless, some species found here are previously reported from the Cretaceous through the Upper Eocene–lower Oligocene, others from the Cretaceous through the Miocene, thus exhibiting a non-random occurrence. Species with an even more limited time-range of occurrence are those thus far found previously only from the Eocene–Oligocene (e.g., *Archaeomonas karinae*, Table 1), only from the Miocene (e.g., *Archaeomonas gratiosa*, Table 1), and the Miocene through the Pliocene. The notable shift in archaeomonad species composition chronicled here coincides with the transitional palaeoceanographic and palaeoclimatic nature of the Oligocene Epoch. We observe that the occurrence of most of our species previously known to science is consistent with their occurrence ranges published from other geographies. This suggests that there may be the potential for index species among the archaeomonad stomatocysts for both regional and wider biostratigraphies. Improvements in species level recognition of the cysts would help such progress, as convincingly argued by Andrén et al. (1999), Kato (2019), and Kato and Suto (2019).

More research attention has been given to the potential of freshwater chrysophyceans for tracking environmental changes (Zeeb and Smol 2002) where well-defined growth optima have been established for many species. Although most chrysophyceans live in a wide range of fresh aquatic

to semiaquatic habitats, a surprising number of species have been found to tolerate higher salinity in inland lakes and brackish coastal and estuarine waters (Mitchell and Silver 1986; Zeeb and Smol 1995; Andrén et al. 1999; Rull and Vegas-Vilarrúbia 2000; Hällfors 2004; Riaux-Gobin et al. 2011). Growth optima have yet to be established for any of the extant marine stomatocysts, apart from tendencies for sea-ice and cold waters of the Antarctic species (Mitchell and Silver 1982, 1986; Riaux-Gobin et al. 2011).

Although an allochthonous origin of some of our stomatocysts cannot be totally disregarded, taking all of our findings into account, we observe that there are several solid arguments for an autochthonous origin of the most of our stomatocysts. First, the majority of stomatocysts recovered are known to science and have been reported in sediments of marine origin. Second, the organic matter contribution is negligible in our diatomites and should have been higher if the stomatocysts were swept to sea from inland sources. Third, only a few diatom genera now known to be exclusively freshwater (e.g., *Aulacoseira*) are only rarely found in our samples, with or without stomatocysts. Fourth, the majority of co-occurring diatoms, pormaleans, silicoflagellates, and ebridians suggest a fundamentally marine depositional basin where the native Rupelian stomatocysts settled in our section of the Central Paratethys.

## Conclusions

The unanticipated species richness of archaeomonad stomatocysts recovered from the deposits of the Futoma Diatomite Member in Southeast Poland was only revealed through SEM re-examination of the material originally studied using LM in the 1970s. The small size of most of the stomatocysts, their even smaller diagnostic features, and their unpredictable occurrence and relative scarcity in marine sediments compared to the other siliceous microfossils (particularly diatoms) may be responsible for them being overlooked in similar studies. The geographic and stratigraphic ranges of known species and diverse flora of species proposed here as new to science suggest that marine archaeomonads carry biostratigraphic and palaeoecological value in both local and broader geological settings. Our work underscores earlier calls for application of modern microscopical techniques in research into this little known type of siliceous microfossil and will hopefully encourage similar examination of diatomaceous deposits around the world.

## Acknowledgements

We thank Konrad Wołowski (KRAM), as well as the administration of the W. Szafer Institute of Botany, PAS, Kraków, Poland, for making this material available to us. The late Janusz Kotlarczyk (1931–2017; AGH) led field expeditions. Two anonymous reviewers provided thoughtful constructive comments and greatly improved the manuscript. Funding

for field work, sample processing and early analyses in the mid- to late 1970s was provided by the AGH and W. Szafer Institute of Botany, PAS in Kraków and the Polish Geological Institute in Warsaw. We appreciate help of the late Jolanta Pająk (1952–2000; KRAM) in processing the sediment samples. Funding for electron microscopy of siliceous microfossils was provided by an NSERC Discovery Grant and the Mount Allison University Marjorie Bell Faculty Fund (Sabbatical) awarded to IK.

Editor: Krzysztof Hryniewicz

## References

- Abe, K., Tsutsui, H., and Jordan, R.W. 2016. *Hyalolithus tumescens* sp. nov., a siliceous scale-bearing haptophyte from the Middle Eocene. *Journal of Micropalaeontology* 35: 143–149.
- Andrén, E., Shimmield, G., and Brand, T. 1999. Environmental changes of the last three centuries indicated by siliceous microfossil records from the southwestern Baltic Sea. *The Holocene* 9: 25–38.
- Bachmann, A. 1964. Fossil Silicoflagellidae und Archaeomonadaceae. In: W. Ichikawa, N. Fuji, and A. Bachmann (eds.), Fossil Diatoms, Pollen Grains and Spores, Silicoflagellates and Archaeomonads in the Miocene Hojuji Diatomaceous Mudstone, Noto Peninsula, Central Japan. *Science Reports of Kanazawa University* 9: 87–118.
- Bai, X., Piątek, J., Wołowski, K., Yang, T., and Chen, X. 2023. Sedimentary chrysophycean stomatocysts from an alpine lake in the Three Gorge Reservoir region, central China. *Nova Hedwigia* 116: 193–230.
- Barss, M.S., Bujak, J.P., and Williams, G.L. 1979. Palynological zonation and correlations of sixty-seven wells, Eastern Canada. *Geological Survey Canada, Geological Survey Papers* 78–24: 1–118.
- Bessudova, A.Y., Larisa, M., Sorokovikova, L.M., Irina, V., Tomberg, I.V., and Likhoshway, Y.V. 2018. Silica-scaled chrysophytes in large tributaries of Lake Baikal. *Cryptogamie, Algologie* 39: 145–165.
- Buck, K.R. and Garrison, D.L. 1983. Protists from the ice-edge of the Weddell Sea. *Deep-Sea Research* 30: 1261–1277.
- Cornell, W.C. 1972. Late Cretaceous chrysomonad cysts. *Palaeogeography, Palaeoclimatology, Palaeoecology* 12: 33–47.
- Cronberg, G. 1986. Chrysophycean cysts and scales in lake sediments: a review. In: J. Kristiansen and R.A. Andersen (eds.), *Chrysophytes: Aspects and Problems*, 281–315. Cambridge University Press, Cambridge.
- Cronberg, G. and Sandgren, C.D. 1986. A proposal for the development of standardized nomenclature and terminology for chrysophycean statospores. In: J. Kristiansen and R. A. Andersen (eds.), *Chrysophytes: Aspects and Problems*, 317–328. Cambridge University Press, Cambridge.
- Deflandre, G. 1932a. Note sur les Archaeomonadacées. *Bulletin de la Société Botanique de France* 79: 346–355.
- Deflandre, G. 1932b. *Litharchaeocystis costata* nov. gen. nov. spec., Chrysophycée marine fossile. Remarques sur les Chrysostomatacées. *Comptes Rendus Hebdomadaires des Séances de l'Académie des Sciences* 194: 1273–1275.
- Deflandre, G. 1932c. Archaeomonadaceae, une nouvelle famille de Protistes fossiles marins à loge siliceuse. *Comptes Rendus Hebdomadaires des Séances de l'Académie des Sciences* 194: 1859–1861.
- Deflandre, G. 1932d. Sur quelques Protistes siliceux d'un sondage de la mer Caspienne. *Bulletin de la Société française de microscopie* 7: 78–81.
- Deflandre, G. 1933. Seconde note sur les Archaeomonadacées. *Bulletin de la Société Botanique de France* 80: 79–90.
- Deflandre, G. 1938. Troisième note sur les Archaeomonadacées. *Bulletin de la Société Française de Microscopie* 7: 73–88.
- Deflandre, G. and Deflandre-Rigaud, M. 1969. *Nannofossiles siliceux I: Archaeomonadaceae: Fichier Micropaléontologique Général – Série 19*. 131 pp. Centre National de la Recherche Scientifique, Paris.
- De Saedeleer, H. 1929. Notules systématiques. VI. *Physomonas*. *Annales de Protistologie* 2: 177–178.
- Duff, K.E. and Smol, J.P. 1989. Chrysophycean stomatocysts from the postglacial sediments of Tasikutaq Lake, Baffin Island, N.W.T. *Canadian Journal of Botany* 67: 1649–1656.
- Duff, K.E. and Smol, J.P. 1991. Morphological descriptions and stratigraphic distributions of the chrysophycean stomatocysts from a recently acidified lake (Adirondack Park, N.Y.). *Journal of Paleolimnology* 5: 73–113.
- Duff, K.E. and Smol, J.P. 1994. Chrysophycean cyst flora from British Columbia (Canada) lakes. *Nova Hedwigia* 58: 353–389.
- Duff, K.E., Zeeb, B.A., and Smol, J.P. 1995. *Atlas of Chrysophycean Cysts, Developments in Hydrobiology* 99. 189 pp. Springer, Dordrecht.
- Ellegaard, M., Moestrup, Ø., Andersen, T.J., and Lundholm, N. 2016. Long-term survival of haptophyte and prasinophyte resting stages in marine sediment. *European Journal of Phycology* 51: 328–337.
- Firsova, A.D., Vorobyova, S.S., and Likhoshway, Y.V. 2012. Chrysophycean stomatocysts in the upper Pleistocene and Holocene sediments from Lake Hovsgol, Northern Mongolia. *International Journal of Geosciences* 3: 664–674.
- Gombos, A.M. 1977. Archaeomonads as Eocene and Oligocene guide fossils in marine sediments. *Initial Reports of the Deep Sea Drilling Project* 36: 689–695.
- Graham, J.E., Wilcox, L.W., and Graham, L.E. 2008. *Algae. 2nd Edition*. 720 pp. Benjamin Cummings, San Francisco.
- Hajós, M. 1968. Diatoms of the Miocene sediments of the Mátraalja Basin [in Hungarian]. *Geologica Hungarica, Series Palaeontologica* 37: 1–401.
- Hajós, M. and Stradner H. 1975. Late Cretaceous Archaeomonadaceae, Diatomaceae, and Silicoflagellatae from the South Pacific Ocean, Deep Sea Drilling Project, Leg 29, Site 275. *Initial Reports of the Deep Sea Drilling Project* 29: 913–1009.
- Hällfors, G. 2004. Checklist of Baltic Sea Phytoplankton species (including some heterotrophic protistan groups). *Baltic Sea Environment Proceedings* 95. 288 pp. Helsinki Commission and Baltic Marine Environment Commission, Helsinki.
- Harwood, D.M. and Gersonde, R. 1990. Lower Cretaceous diatoms from ODP Leg 113 Site 693 (Weddell Sea). Part 2: Resting spores, Chrysophycean cysts, and endoskeletal dinoflagellate, and notes on the origin of diatoms. *Proceedings of the Ocean Drilling Program, Scientific Results* 113: 403–425.
- Holen, D.A. 2014. Chrysophyte stomatocyst production in laboratory culture and descriptions of seven cyst morphotypes. *Phycologia* 53: 426–432.
- Kaczmarzka, I. 1982. Diatoms of the two Lower Oligocene diatomites from the Polish Carpathian Flysch. *Acta Geologica Academiae Scientiarum Hungaricae* 25: 39–47.
- Kaczmarzka I. and Ehrman, J.M. 2023. Parmalean and other siliceous nanofossils from the Oligocene of Polish Flysch Carpathians. *Acta Palaeontologica Polonica* 68: 441–456.
- Kato, Y. 2019. Late Miocene and Pliocene fossil chrysophyte cysts from ODP Site 689 and DSDP Site 513, the Atlantic sector of the Southern Ocean. *Nova Hedwigia, Beiheft* 148: 131–156.
- Kato, Y. and Suto, I. 2019. Fossil chrysophyte cysts as potentially useful paleoceanographic indicators: comparison with Southern Ocean diatom assemblages. *Nova Hedwigia, Beiheft* 148: 113–129.
- Kotlarczyk, J. 1982. Role of diatoms in sedimentation and biostratigraphy of the Polish Flysch Carpathians. *Acta Geologica Academiae Scientiarum Hungaricae* 25: 9–21.
- Kotlarczyk J. and Kaczmarzka, I. 1987. Two diatom horizons in the Oligocene and (?) Lower Miocene of the Polish Outer Carpathians. *Annales Societatis Geologorum Poloniae* 57: 143–188.
- Kotlarczyk, J. and Leśniak, T. 1990. *Lower Part of the Menilite Formation and Related Futoma Diatomite Member in the Skole Unit of the Polish Carpathians*. 74 pp. Wydawnictwo Akademii Górniczo-Hutniczej, Kraków.
- Kotlarczyk J., Jerzmańska, A., Świdnicka, E., and Wiszniowska, T. 2006. A framework of ichthyofaunal ecostratigraphy of the Oligocene–Early Miocene strata of the Polish Outer Carpathian basin. *Annales Societatis Geologorum Poloniae* 76: 1–111.
- Kotlarczyk, J. and Uchman, A. 2012. Integrated ichnology and ichthyology of the Oligocene Menilite Formation, Skole and Subsilesian nappes, Polish Carpathians: A proxy to oxygenation history. *Palaeogeography, Palaeoclimatology, Palaeoecology* 331: 104–118.
- Kristiansen, J. and Andersen, R.A. 1986. *Chrysophytes: Aspects and Problems*. 352 pp. Cambridge University Press, Cambridge.



- Ling, H.Y. and Kim, B.K. 1983. Miocene Archaeomonads from Pohang Area, Korea. *The Journal of the Geological Society of Korea* 19: 247–251.
- Lipps, J.H. (ed.) 1993. *Fossil Prokaryotes and Protists*. 342 pp. Blackwell Scientific Publications, Boston.
- Lipps, J.H. and McCartney, K. 1993. Chrysophytes. In: J.H. Lipps (ed.), *Fossil Prokaryotes and Protists*, 141–154. Blackwell Scientific Publications, Boston.
- Mitchell, J.G. and Silver, M.W. 1982. Modern archaeomonads indicate sea-ice environments. *Nature* 296: 437–439.
- Mitchell, J.G. and Silver, M.W. 1986. Archaeomonad (Chrysophyta) cysts: ecological and paleoecological significance. *BioSystems* 19: 289–298.
- Nygaard, G. 1956. Ancient and recent fora of diatoms and chrysophyceae in Lake Gribso. *Folia Limnologica Scandinavica* 8: 32–94.
- Perch-Nielsen, K. 1975. Late Cretaceous to Pleistocene archaeomonads, ebridians, endoskeletal dinoflagellates, and other siliceous microfossils from the Subantarctic Southwest Pacific, DSDP, Leg 29. *Initial Reports of the Deep Sea Drilling Project* 29: 873–907.
- Perch-Nielsen, K. 1978. Eocene to Pliocene archaeomonads, ebridians, and endoskeletal dinoflagellates from the Norwegian Sea, DSDP Leg 38. *Initial Reports of the Deep Sea Drilling Project* 38-41, Supplement 15: 147–175.
- Piątek, J. 2017. A morphotype-rich assemblage of chrysophycean stomatocysts in mountain lakes in the Cameroon Highlands, Africa. *Cryptogamie, Algologie* 38: 159–180.
- Rampì, L. 1940. Archaeomonadaceae del cretaceo Americano. *Atti della Società Italiana delle Scienze Naturali* 79: 60–68.
- Rampì, L. 1948. Su alcune Archaeomonadaceae (Crisomonadine fossili marine) nuove od interessanti. *Atti della Società Italiana delle Scienze Naturali* 87: 185–188.
- Rampì, L. 1969. Archaeomonadacées de la Diatomite Eocène de Kreyenhagen, Californie. *Cahiers de Micropaléontologie, Série I* 14: 1–11.
- Riaux-Gobin, C. and Stumm, K. 2006. Modern Archaeomonadaceae from the land-fast ice off Adélie Land, East Antarctica: a preliminary report. *Antarctic Science* 18: 51–60.
- Riaux-Gobin, C., Poulin, M., Dieckmann, G., Labruné, C., and Vétion, G. 2011. Spring phytoplankton onset after the ice break-up and sea-ice signature (Adélie Land, East Antarctica). *Polar Research* 30: 5910.
- Rull, V. and Vegas-Vilarrúbia, T. 2000. Chrysophycean stomatocysts in a Caribbean mangrove. *Hydrobiologia* 428: 145–150.
- Sachsenhofer, R.F., Popov, S.V., Bechtel, A., Coric, S., Francu, J., Gratzner, R., Grunert, P., Kotarba, M., Mayer, J., Pupp, M., Rupprecht, B.J., and Vincent, S.J. 2017. Oligocene and Lower Miocene source rocks in the Paratethys: palaeogeographical and stratigraphic controls. In: M.D. Simmons, G.C. Tari, and A.I. Okay (eds.), *Petroleum Geology of the Black Sea*. Geological Society, London, Special Publications 464: 267–306.
- Salata D. and Uchman, A. 2019. New interpretation of the provenance of crystalline material from Oligocene flysch deposits of the Skole Nappe, Poland: evidence from heavy minerals and clasts in the Nowy Borek section. *Geologos* 25: 163–174.
- Sandgren, C.D. 1988. *Growth and Reproductive Strategies of Freshwater Phytoplankton*. 442 pp. Cambridge University Press, Cambridge.
- Siver, P.A. 2020. Remarkably preserved cysts of the extinct synurophyte, *Mallomonas ampla*, uncovered from a 48 Ma freshwater Eocene lake. *Scientific Reports* 10: 5204.
- Stradner, H. 1971. On the ultrastructure of Miocene Archaeomonadaceae (phytoflagellates) from Limberg, Lower Austria. In: A. Farinacci (ed.), *Proceedings of the Second Plankton Conference, Roma*, 1183–1199. Tecnoscienza, Rome.
- Stickley, C.E., Koç, N., Brumsack, H.-J., Jordan, R.W., and Suto, I. 2008. A siliceous microfossil view of Middle Eocene Arctic paleoenvironments: A window of biosilica production and preservation. *Paleoceanography* 23: PA1S14.
- Takahashi, E., Watanabe, K., and Satoh, H. 1986. Siliceous cysts from Kita-No-Seto Strait, north of Syowa Station, Antarctica. *Memoirs of National Institute of Polar Research, Special Issue* 40: 84–95.
- Turland, N.J., Wiersema, J.H., Barrie, F.R., Greuter, W., Hawksworth, D.L., Herendeen, P.S., Knapp, S., Kusber, W.-H., Li, D.-Z., Marhold, K., May, T.W., McNeill, J., Monro, A.M., Prado, J., Price, M.J., and Smith, G.F. 2018. *International Code of Nomenclature for Algae, Fungi, and Plants (Shenzhen Code) adopted by the Nineteenth International Botanical Congress Shenzhen, China, July 2017*. *Regnum Vegetabile* 159. 201 pp. Koeltz Botanical Books, Glashütten.
- Tynan, E.J. 1960. The Archaeomonadaceae of the Calvert Formation (Miocene) of Maryland. *Micropaleontology* 6: 33–39.
- Tynan, E.J. 1971. Geologic occurrence of the Archaeomonads. In: A. Farinacci (ed.), *Proceedings of the Second Plankton Conference, Roma*, 1225–1230. Tecnoscienza, Rome.
- VanLandingham, S.L. 1964. Chrysophyta cysts from the Yakima Basalt (Miocene) in south central Washington. *Journal of Paleontology* 38: 729–739.
- Van de Vijver, B. and Beyens, L. 2000. Chrysophycean stomatocysts from freshwater habitats of the Strømness Bay area, South Georgia, Antarctica. *Canadian Journal of Botany* 78: 88–97.
- Wilkinson, A.N., Roland, I., Hall, R.I., and Smol, J.P. 1999. Chrysophyte cysts as paleolimnological indicators of environmental change due to cottage development and acidic deposition in the Muskoka-Haliburton region, Ontario, Canada. *Journal of Paleolimnology* 22: 17–39.
- Wilkinson, A.N., Zeeb, B.A., and Smol, J.P. 2001. *Atlas of Chrysophycean Cysts*. Vol. 2. 169 pp. Kluwer Academic Publishers, Dordrecht.
- Yoshida, M., Noël, M.H., Nakayama, T., Naganuma, T., and Inouye, I. 2006. A haptophyte bearing siliceous scales: ultrastructure and phylogenetic position of *Hyalolithus neolepis* gen. et sp. nov. (Prymnesiophyceae, Haptophyta). *Protist* 157: 213–234.
- Zeeb, B.A. and Smol, J.P. 1991. Paleolimnological investigation of the effects of road salt seepage on scaled chrysophytes in Fonda Lake, Michigan. *Journal of Paleolimnology* 5: 263–266.
- Zeeb, B.A. and Smol, J.P. 1993. Chrysophycean stomatocyst flora from Elk Lake, Clearwater County, Minnesota. *Canadian Journal of Botany* 71: 737–756.
- Zeeb, B.A. and Smol, J.P. 1995. A weighted-averaging regression and calibration model for inferring lakewater salinity using chrysophycean stomatocysts from lakes in western Canada. *International Journal of Salt Lake Research* 4: 1–23.
- Zeeb, B.A. and Smol, J.P. 2002. Chrysophyte scales and cysts. In: J.P. Smol and H.J.B. Birks (eds.), *Tracking Environmental Change Using Lake Sediments Volume 3: Terrestrial, Algal, and Siliceous Indicators*, 203–223. Kluwer Academic Publishers, Dordrecht.
- Zeeb, B.A., Duff, K.E., and Smol, J.P. 1990. Morphological descriptions and stratigraphic profiles of the chrysophycean stomatocysts from the recent sediments of Little Round Lake, Ontario. *Nova Hedwigia* 51: 361–380.
- Zhang, W., Yang, H., Xia, X., Xie, L., and Xie, G. 2016. Triassic chrysophyte cyst fossils discovered in the Ordos Basin, China. *Geology* 44: 1031–1034.